PHILOSOPHICAL TRANSACTIONS B

royalsocietypublishing.org/journal/rstb

Research

Cite this article: Dong L, Wang Y-Q, Zhao Q, Vasilyan D, Wang Y, Evans SE. 2022 A new stem-varanid lizard (Reptilia, Squamata) from the early Eocene of China. *Phil. Trans. R. Soc. B* **377**: 20210041.
https://doi.org/10.1098/rstb.2021.0041

Received: 18 June 2021
Accepted: 22 October 2021

One contribution of 11 to a theme issue 'The impact of Chinese palaeontology on evolutionary research'.

Subject Areas:
evolution, palaeontology

Keywords:
early Eocene, China, Varanidae, evolution

Author for correspondence:
Liping Dong
e-mail: dongliping@ivpp.ac.cn

Electronic supplementary material is available online at https://doi.org/10.6084/m9.figshare.c.5772146.

THE ROYAL SOCIETY PUBLISHING

A new stem-varanid lizard (Reptilia, Squamata) from the early Eocene of China

Liping Dong[1,2], Yuan-Qing Wang[1,2], Qi Zhao[1,2], Davit Vasilyan[3,4], Yuan Wang[1,2] and Susan E. Evans[5]

[1]Key Laboratory of Vertebrate Evolution and Human Origins, Institute of Vertebrate Paleontology and Paleoanthropology, Chinese Academy of Sciences, Beijing, People's Republic of China
[2]CAS Center for Excellence in Life and Paleoenvironment, Beijing, People's Republic of China
[3]JURASSICA Museum, Porrentruy, Switzerland
[4]Department of the Geosciences, University of Fribourg, Fribourg, Switzerland
[5]Centre for Integrative Anatomy, Department of Cell and Developmental Biology, University College London, London, UK

LD, 0000-0001-9152-0359

Monitor lizards (genus *Varanus*) are today distributed across Asia, Africa and Australasia and represent one of the most recognizable and successful lizard lineages. They include charismatic living species like the Komodo dragon of Indonesia and the even larger extinct *Varanus prisca* (*Megalania*) of Australia. The fossil record suggests that living varanids had their origins in a diverse assemblage of stem (varaniform) species known from the Late Cretaceous of China and Mongolia. However, determining the biogeographic origins of crown-varanids has proved problematic, with Asia, Africa and Australia each being proposed. The problem is complicated by the fragmentary nature of many attributed specimens, and the fact that the most widely accepted, and most complete, fossil of a stem-varanid, that of *Saniwa ensidens*, is from North America. In this paper, we describe a well-preserved skull and skeleton of a new genus of stem-varanid from the Eocene of China. Phylogenetic analysis places the new genus as the sister taxon of *Varanus*, suggesting that the transition from Cretaceous varaniform lizards to *Varanus* occurred in East Asia before the origin and dispersal of *Varanus* to other regions. The discovery of the new specimen thus fills an important gap in the fossil record of monitor lizards. The similar lengths of the fore- and hindlimbs in this new taxon are unusual among the total group Varanidae and suggest it may have had a different lifestyle, at least from the contemporaneous North American *S. ensidens*.

This article is part of the theme issue 'The impact of Chinese palaeontology on evolutionary research'.

1. Introduction

The lizard family Varanidae encompasses more than 80 living *Varanus* species [1] currently distributed across Africa, Asia and Australia, and a few close fossil relatives. These lizards have long intrigued both researchers and amateur enthusiasts. Despite having a relatively conservative morphology, *Varanus* is unusual in showing high taxonomic and ecological diversity within a single genus (albeit within several subgenera [2,3]), as well as the widest range of body sizes of any extant lizard clade, from 0.12 m to 1.6 m (snout-vent length (SVL)) [1,4]. In addition to the extant Komodo dragon (*Varanus komodoensis*: total length (TL) including tail approximately 3 m), *Varanus* also includes the extinct Australian *Varanus prisca* [=*Megalania*], the largest known terrestrial lizard with an estimated TL of up to 5 m [5]. Among living species, the Bornean earless monitor *Lanthanotus borneensis* is the sister taxon to *Varanus* [6,7].

There is a general consensus that Varanidae had its roots in Eurasia among the varaniforms (*sensu* [6], see below) of the Late Cretaceous [8–10], with several well-preserved fossil varaniforms known from the Campanian deposits of the Gobi Desert [11–14]. The origin of the true monitor *Varanus* is more controversial, with Asian, African and Gondwanan origins having been proposed [10].

Many early records of *Varanus* are from the early Neogene of Europe and northern Africa, represented mostly by isolated vertebrae, except *Varanus rusingensis* (Miocene, Kenya [15]), *Varanus mokrensis* (Miocene, Czech Republic [16]) and *Varanus marathonensis* (Miocene, Greece [5]; Miocene, Spain [17]) (figure 3*b*). The Palaeogene temporal gap between the Late Cretaceous varaniforms and the first Neogene records of *Varanus* is therefore a key period in the evolution of true monitors. However, the only definitive stem-varanid material from this era is that of *Saniwa ensidens*. Although this species is represented by several skeletons from North America [18,19], Palaeogene varanid fossils are mostly isolated vertebrae, such as stem-*Varanus* vertebrae reported from the early Oligocene of Egypt [20,21] and *Saniwa* vertebrae from the middle Eocene of Mongolia [22].

The Palaeogene fossil record of varaniforms from China is very poor, with only a dentary and a series of vertebrae (Varaniformes, gen et sp. indet.) reported from the Palaeocene of Qianshan locality, Anhui Province [23]. Herein, we describe a well-preserved skull and skeleton of a new stem-varanid that was collected in 2008 by a field team of the Palaeogene mammal research group of the Institute of Vertebrate Paleontology and Paleoanthropology, Chinese Academy of Sciences (IVPP, CAS), from the Lower Eocene Yuhuangding Formation at the Dajian locality, Liguanqiao Basin, China. This specimen is important in showing that stem-varanids were present in Asia as well as Euramerica in the Palaeogene.

2. Geological background

The lizard specimen, IVPP V 22770, was found at the Dajian locality, which is located about 47.5 km northeast of Shiyan City and lies in Xijiadian Township, Danjiangkou City, Hubei Province (electronic supplementary material, figure S1). The Liguanqiao Basin, where the Dajian locality occurs, exposes deposits from the Late Cretaceous to Neogene. The Eocene deposits are widely distributed and divided into the Yuhuangding, Dacangfang and Hetaoyuan formations in ascending order [24]. The lizard fossil was recovered from the middle one of the three fossiliferous horizons within the Yuhuangding Formation and is early Eocene in age [24,25]. There is no absolute dating for the horizon, but the same horizon has yielded abundant mammal remains, including *Rhombomylus turpanensis*, *Advenimus hupeiensis*, *Asiocoryphodon conicus* and *Danjiangia pingi*, which suggests a late early Eocene age [24,26]. The palaeoclimatic conditions below the first fossiliferous horizon in the middle member of the Yuhuangding Formation have been carefully reconstructed based on the presence of the Palaeocene-Eocene Thermal Maximum, when it was warm and humid with increased precipitation [27–29]. However, the locality was within the broad arid belt in the Eocene [30] although no relevant data have been obtained from the lizard-bearing horizon itself.

3. Material and methods

The lizard specimen (IVPP V 22770) is a relatively complete skeleton in which the postcranial elements are mostly disarticulated and scattered in a limited mass within a reddish siltstone block (figure 1*a*). The skull, originally preserved in ventral view, was carefully prepared off the main block to expose the dorsal surface and to permit a high-resolution computerized tomography (CT) scan (figure 2; electronic supplementary material, figures S2 and S3). Two articulated trunk vertebrae were also prepared free from the block (electronic supplementary material, figures S2 and S8A) to obtain detailed morphological information and for CT scanning. The specimen is deposited in the collection of the IVPP, CAS.

(a) High-resolution computerized tomography

The skull was scanned twice at the Key Laboratory of Vertebrate Evolution and Human Origins of the Chinese Academy of Sciences (KLVEHO, CAS), once for the whole skull and then again for the braincase. It was then rescanned at the Yinghua Inspection and Testing Centre to yield higher resolution images. The two vertebrae were also scanned at the KLVEHO, CAS to reveal the anatomy of the articulation between the vertebrae. See the electronic supplementary material, text S1 for the detailed scan parameters.

The reconstructed slices were processed in Avizo 9.1 (Thermo Fisher Scientific Inc.) to visualize the slice data and segment the bony elements of interest. Snapshots were then taken from rendered images of the skull, the braincase and the vertebrae. The surface data from several separate fragments of one vertebra was reconstructed in Avizo 9.1 to give a better view of the vertebra as well as to provide more accurate measurements.

(b) Histological sections of ribs and fibula

Histological sections were sampled from the mid diaphysis of the right fibula and the proximal parts of two ribs from specimen IVPP V 22770 (electronic supplementary material, figure S2 for the sample positions). Another section was also made from the distal part of the rib of a commercially obtained specimen of *Varanus*, stated to be *Varanus salvator*, which was of approximately the same body size (84 mm skull length) as the fossil specimen, and whose astragalocalcaneum still displayed a clear suture. Sections were made using the EXAKT-Cutting-Grinding System at the KLVEHO, CAS (see the electronic supplementary material, text S2 for the detailed process), and then viewed and photographed using a Zeiss PromoTech microscope.

(c) Comparative osteology

Comparative skeletal material of *Varanus* was examined at the Natural History Museum, London (NHM, London) and the Natural History Museum, Basel. These observations were supplemented by digital CT data on the Digimorph website, University of Texas, Austin (http://digimorph.org/index.phtml) and MorphoSource (https://www.morphosource.org), and CT scan data of a *Lanthanotus* specimen in the collections of the Kanagawa Prefectural Museum of Natural History, Japan. A full list of specimens examined can be found in the electronic supplementary material, table S1.

(d) Nomenclatural usage

For clarity, we are using Varanidae in the restricted sense of *Varanus* and those fossil taxa more closely related to it than to *Lanthanotus*. Lanthanotidae is the sister taxon to Varanidae and encompasses *Lanthanotus* and fossil taxa more closely related to it than to *Varanus* (e.g. *Cherminotus*, [6,10]). Varaniformes (*sensu* [6]) encompasses anguimorphs more closely related to *Varanus* than to *Anguis*,

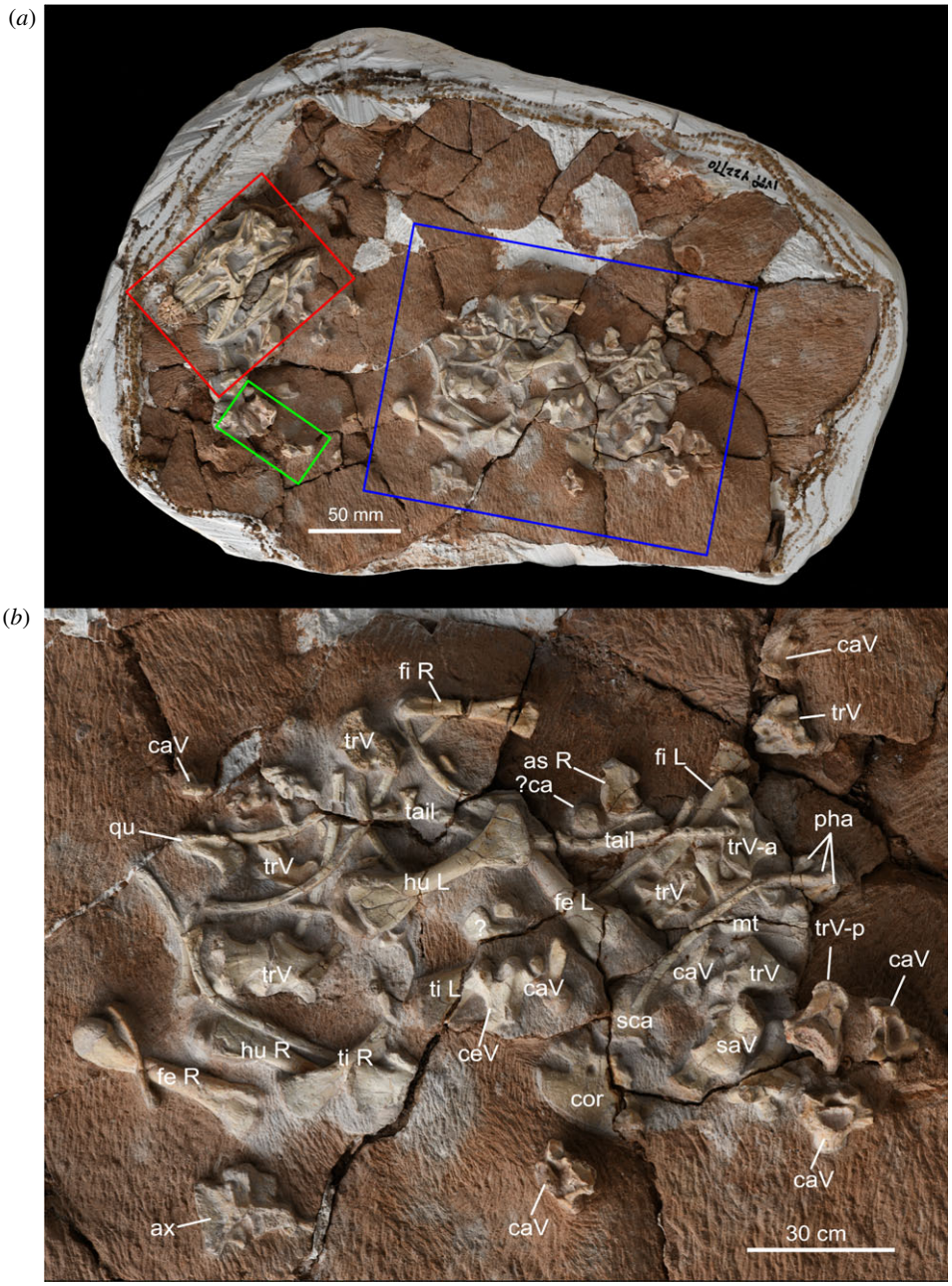

Figure 1. Photograph (*a*) of the holotype specimen IVPP V 22770 of *Archaeovaranus lii* and a close-up of the postcranial skeleton (*b*). The blue rectangle in (*a*) indicates the area present in (*b*); the red rectangle indicates the part present in the electronic supplementary material, figure S4A; the green rectangle indicates the part shown in the electronic supplementary material, figure S4D. Abbreviations: as, astragalus; ax, axis; ca, calcaneus; caV, caudal vertebra; ceV, cervical vertebra; cor, coracoid; fe, femur; fi, fibula; hu, humerus; L, left; mt, metatarsal; pha, phalanx; qu, quadrate; R, right; saV, sacral vertebra; sca, scapula; ti, tibia; trV, trunk vertebra; trV-p, posterior trunk vertebra.

Heloderma or *Xenosaurus*. We avoid Varanoidea because as used in traditional morphology-based phylogenies this encompasses *Heloderma* as well as *Lanthanotus* and *Varanus*, whereas molecular phylogenies (e.g. [9]) place *Heloderma* closer to Anguidae (within Neoanguimorpha) than to varanids. This is important as it suggests morphological characters shared by *Heloderma* (e.g. posteriorly extended—'retracted'—external narial opening, sharply recurved teeth, broad-based teeth with a shallow implantation and plicidentine) and varaniforms have evolved independently and should be treated with caution in comparisons.

(e) Phylogenetic analysis

To explore the position of *Archaeovaranus* within Squamata generally, we first coded it into the morphological matrix of Gauthier *et al*. [7] and ran two analyses, one unconstrained and one constrained by a molecular backbone (see the electronic supplementary material, text S3). Having confirmed the placement of *Archaeovaranus* within Anguimorpha, we then coded it into the more focused dataset of Villa *et al*. [17], as modified from Conrad *et al*. [31], using the character ordering of Conrad *et al*. [31] and the matrix amendments of Villa *et al*. [17] (see the electronic supplementary material, text S3 for a detailed explanation). We replaced the coding of '*Saniwa*' *feisti* in the original matrix with data from the recent redescription of that species as *Palaeonecrosaurus feisti* by Smith & Habersetzer [32], and we added codings for *Heloderma suspectum* and *Eosaniwa kuhni*. The resulting full matrix had 496 morphological characters, 5729 molecular characters and 88 taxa (operational taxonomic units) (electronic supplementary material, data S1). *Shinisaurus* was the designated outgroup for four analyses, as it is now considered the sister taxon to *Lanthanotus*+*Varanus* among extant squamates (e.g. [33]), but we also ran four analyses with *Heloderma* as the outgroup.

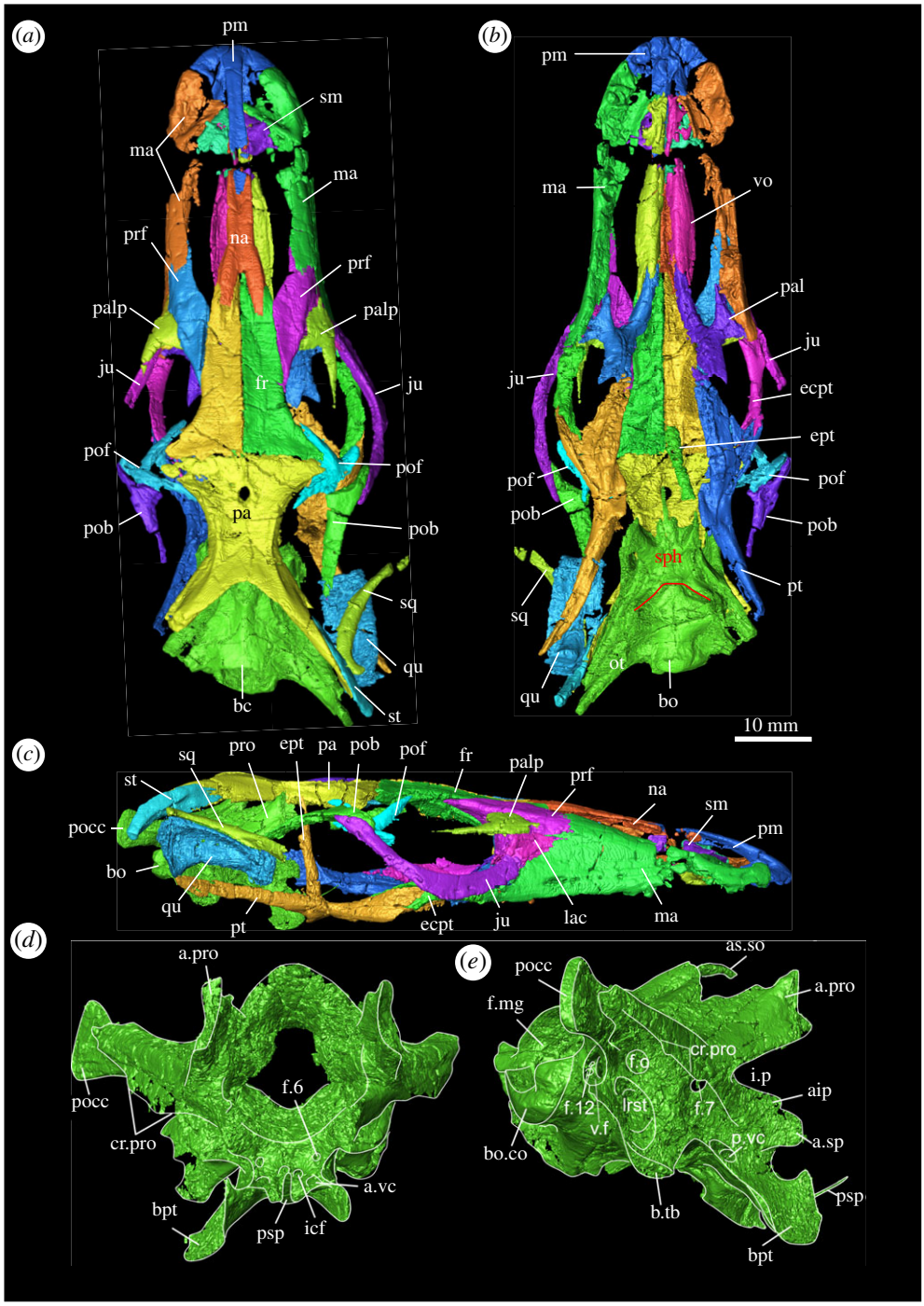

Figure 2. The cranium of the *Archaeovaranus lii* holotype (IVPP V 22770): three-dimensional renders in dorsal (*a*), ventral (*b*) and lateral (*c*) views; three-dimensional renders of the braincase in anterior (*d*) and posterolateral (*e*) views. (*d*) and (*e*) are not to scale. Abbreviations: aip, anterior inferior process of prootic; as.so, ascending process of supraoccipital; a.pro, alar process of prootic; a.sp, alar process of sphenoid; a.vc, anterior opening of vidian canal; bc, braincase; bo, basioccipital; bo.co, basioccipital condyle; bpt, basipterygoid; b.tb, basal tubercle; cr.pro, crista prootica; ecpt, ectopterygoid; ept, epipterygoid; f.6, foramen for abducens nerve; f.7, foramen for facial nerve; f.12, foramen for hypoglossal nerve; f.mg, foramen magnum; fr, frontal; f.o, fenestra ovalis; icf, internal carotid foramen; i.p, incisura prootica; ju, jugal; lac, lacrimal; lrst, lateral opening of recessus scalae tympani; ma, maxilla; na, nasal; ot, otooccipital; pa, parietal; pal, palatine; palp, palpebral; pm, premaxilla; pocc, paroccipital process; pob, postorbital; pof, postfrontal; prf, prefrontal; pro, prootic; psp, parasphenoid; pt, pterygoid; p.vc, posterior opening of vidian canal; qu, quadrate; sm, septomaxilla; sph, sphenoid; sq, squamosal; st, supratemporal; v.f, vagus foramen; vo, vomer.

Parsimony analyses were then conducted in TNT v. 1.5 [34], using the New Technology search with sectorial search, ratchet, drift and fusion options activated (default settings) and a minimum length tree to be found in 20 replicates. Each of the analyses was run with the full combined dataset (to ensure the correct positioning of extant taxa), then with the morphological dataset alone. In the analyses using only morphological data, we deactivated a subset of taxa represented by mainly molecular data. We also ran the analyses with or without the marine dolichosaur taxa, as there is a lack of consensus as to their position (or that of Mosasauria as a whole) within Squamata (e.g. [7]) (see the electronic supplementary material, text S3 for further explanation).

4. Systematic palaeontology

Squamata Oppel, 1811
Anguimorpha Fürbringer, 1900
Varanidae Merrem, 1820
Archaeovaranus lii gen. et sp. nov.

Etymology. The generic name Archaeo- reflects the primitive phylogenetic position of this lizard in the evolution of Varanidae, and -varanus suggests the close relationship with the genus *Varanus*, whereas the specific name lii honours the late Prof. Chuankui Li for his important work on Palaeogene mammals, including some from the same locality as the holotype lizard described herein.

Holotype. IVPP V 22770, a nearly complete skeleton with an intact skull and associated but mostly disarticulated postcranial elements (figure 1*a*).

Locality and horizon. Dajian locality (IVPP fossil site catalogue number 76006, see Ma et Chen, [24]) (32°46′19.74° N, 111°12′33.0° E), about 35 km northwest of Danjiangkou City, Hubei Province, China; Middle Member, Yuhuangding Formation (early Eocene; 52–56 Ma; the palaeomagnetic study suggesting a precise age of 53 Ma for the fossil-bearing horizon [24,25,35]).

Diagnosis. The new genus and species is a medium-sized stem-varanid that resembles *S. ensidens* and *Varanus* and differs from helodermatids, palaeovaranids, lanthanotids and the Late Cretaceous stem-varanids in combining the following characters: posteriorly extended (retracted) external narial openings that reach frontals; a single median nasal; two lacrimal foramina, the ventral of which is fully enclosed by the lacrimal; elongated vomers; a U-shaped palatine; a short maxillary tooth row mostly confined to preorbital region, bearing well-spaced recurved teeth with basal plicidentine; intramandibular joint; splenial positioned anterior to level of dorsal prominence of the coronoid; anterior process of coronoid long; and distinct precondylar constriction on the vertebral centra. *Archaeovaranus* resembles *S. ensidens* and differs from *Varanus* in having cristae cranii of frontal separated in ventral midline, separate postfrontal and postorbital, a complete bony postorbital bar, teeth on palatine and pterygoid, posterolaterally placed basal tubera on basioccipital and a single coracoid emargination. It differs from *S. ensidens* in having a longer rostrum, two pterygoid tooth rows (versus a single row), and resembles *Varanus* but not *Saniwa* in having a dorsal lacrimal foramen enclosed by the prefrontal and lacrimal (rather than being restricted to the lacrimal). *Archaeovaranus* differs from both *S. ensidens* and known species of *Varanus* in having the forelimb and hindlimb, and the humerus and femur, of near equal length.

5. Description

The holotype and only specimen, IVPP V 22770 (figure 1*a*), is a nearly complete skeleton, in which the skull is almost intact but the postcranial elements are mostly disarticulated and scattered within the siltstone block. Judging by the visible skeletal growth lines in sections of the right fibula, the animal was probably an adult of about 16 years old at death (see below). However, there is evidence that the animal was still growing. Whereas complete fusion of the long bone epiphyses has occurred at the proximal end of some bones (humerus, femur), it is lacking at the distal ends of the same bones. This asynchronous fusion has also been reported in *Varanus* [36].

The description that follows is based on first-hand examination of the specimen as well as the three-dimensional renders of the skull and sampled vertebrae from the CT data.

(a) Cranium and mandibles

The skull is mostly articulated and was preserved on the edge of the block (figure 1*a*). During collection in the field, the anterior part of the snout (partial premaxillae, maxillae and vomers) had detached from the rest of the skull but was replaced when the skull was prepared off the block (the missing part is very limited, and the distance between the snout tip and the rest of the skull was estimated based on the shape of the vomer and premaxillary nasal process). The left side of the skull was already broken when the skeleton was recovered; the left palpebral bone, jugal, postorbital, parietal, pterygoid and paroccipital process are partly broken, and the squamosal and supratemporal bones are completely missing. The left quadrate was detached from the skull and lay among the postcranial elements (figure 1*b*). The two lower jaws are in articulation at the symphysis but are slightly displaced from the cranium. The left mandible preserves only the dentary and the coronoid *in situ* in lateral view; the displaced postdentary elements are partially preserved in medial view and located below and left of the skull (figure 1*a*). There is a section missing from the postdentary region (electronic supplementary material, figure S4D). The right mandible is preserved in medial view and is nearly complete, with the retroarticular process missing (figure 1*a*; electronic supplementary material, figure S4A). Neither of the mandibles could be removed from the block for scanning as this would have damaged the adjoining bones.

The cranium (figure 2; electronic supplementary material, figure S3) is depressed dorsoventrally, even allowing for some taphonomic compression. The skull roof is generally smooth except for an area of vermiform or 'worm-like' sculpture around the frontoparietal suture [37]. The mid-frontal suture is raised into a ridge that continues onto the parietal, up to the parietal foramen. The snout is elongated, but not strongly tapering, and the external narial openings are posteriorly extended (retracted) so that the nasals and prefrontals are fully separated and the frontal enters the external narial margin. This resembles the condition in *Varanus* and *S. ensidens*, but the external narial opening barely reaches the frontal in *Lanthanotus*, and fails to reach it in *Ovoo* [14], *Paranecrosaurus* [32] or *Heloderma*. The orbit is closed posteriorly by the jugal and postfrontal. The borders of the supratemporal fenestra are completed laterally by the postorbital and squamosal. The braincase is largely exposed in dorsal view (figure 2*a*; electronic supplementary material, figure S3B). As in *Varanus*, the tooth row is almost confined to the preorbital region, with the last maxillary tooth at or only slightly beyond the anterior extremity of the orbit (figure 2*c*). In ventral view, the palate is fully neochoanate, with the vomeronasal opening completely separated from the choana. The suborbital fenestra is moderate in size, and the maxilla was excluded from the borders of the fenestra. The interpterygoid vacuity reaches anteriorly at least halfway between the vomers, and it gradually widens posteriorly. No trace of cranial osteoderms is preserved on the specimen.

The single premaxilla (figure 2; electronic supplementary material, figure S3, S5A) is complete. Four pointed pleurodont teeth are preserved along with its alveolar border, but allowing for empty alveoli, the original premaxillary tooth count was probably eight (7–9 in *Varanus*, see [38]). A long nasal process arises from the alveolar lamina and extends

posteriorly rather than posterodorsally. A small foramen for medial ethmoidal branches of ophthalmic and ethmoidal nerves and the ethmoidal artery [39] perforates the base of the nasal process on each side, as in *S. ensidens* [19], but there is no sign of the foramina present on the anterodorsal surface of the alveolar lamina as in *Varanus*. In dorsal view, the nasal process is moderately broad, and only slightly dilated where it contacts the nasal. The process extends to, or just beyond, the midpoint of the external narial openings, forming the anterior half of the internarial bar, but it does not meet the frontals below the nasals. The process is roughly triangular in transverse section anteriorly, but becomes T-shaped posteriorly with the vertical ventral lamina sandwiched between the two anterior laminae of the nasals. The tapering posterior tip of the process is again triangular in cross-section and is supported from below by the already fused nasals. The palatal plate of the premaxilla is well developed and divides posteriorly into two processes, each of which meets the maxilla and the anterior end of the vomer. The palatal plate bears an anteromedian incisive process composed of two crescentic halves. Laterally, the premaxilla is slightly overlapped by the premaxillary process of the maxilla, enclosing a small premaxillary-maxillary aperture.

The right maxilla (figure 2*c*; electronic supplementary material, figure S5B) is almost complete, whereas the left one (electronic supplementary material, figure S3D) has lost much of the alveolar plate as well as the teeth. The maxilla, in general, is long, low and subtriangular in shape. The long premaxillary process is horizontal and gradually broadens anteriorly as seen in dorsal view. The anteromedial margin of the process is slightly concave and contributes to the formation of a small premaxillary-maxillary aperture. There is a triangular depression on the dorsal surface of the premaxillary process, with distinct lateral and more pronounced medial ridges. The medial ridge forms a lateral support for the septomaxilla and is perforated posteromedially by a foramen for the maxillary nerve and artery [39]. Further posteriorly, the maxilla expands very gradually, forming the oblique anterodorsal margin of the facial process. The low facial process curves inwards and contributes to the skull roof, with the horizontal posterior tip well separated from the nasal and the frontal by the prefrontal. Although Rieppel & Grande [19] thought the medial curvature of the facial process differentiated *S. ensidens* from *Varanus*, a similar curvature does occur in some *Varanus* species (e.g. *Varanus prasinus*, UF-H-77411; *Varanus flavescens*, [2]), and the facial process can extend further medially and posteriorly to approach the frontal (some *Varanus niloticus*, e.g. BMNH 97.5.31.2). The posterior margin of the facial process is more steeply inclined than the anterior one and bears a small projection at the level of the prefrontal–lacrimal suture. A similar projection is located in this position in some *Varanus* (*Varanus salvator*: BMNH 1972.2160; *Varanus bengalensis*: BMNH 1974.2479), but not all species (e.g. *Varanus gouldii*: BMNH 1983.1132). The facial process overlaps the prefrontal extensively, as well as a small portion of the lacrimal. The posterior jugal process is short, with all but the last maxillary tooth positioned anterior to the orbit. This contrasts with *S. ensidens* in which, two or three maxillary teeth have a suborbital position [19]. In ventral view, the maxillary palatal shelf is well-developed anteriorly, narrows gradually into a low medial ridge posterior to the midpoint of the maxilla and then expands slightly where the maxilla meets the palatine. The broad anterior part of the shelf flares ventrally and may originally have met or almost met its counterpart in the midline. Just behind the anteromost articulation with the vomer, there is an additional contact between the maxillary palatal shelf and the vomer, separating the vomeronasal fenestra from the choana (neochoanate palate). Posteriorly, the maxilla is excluded from the margin of the suborbital fenestra by the contact of the palatine and ectopterygoid, as in *Varanus*, *Lanthanotus* and *S. ensidens*, but also *P. feisti* [32] and *Heloderma*. Dorsal to the palatal shelf, the opening of the infraorbital canal, for the nervus alveolaris superior and maxillary artery [39], lies at the anterior extremity of the maxillary–palatine articulation; posterior to this articulation, the maxilla contacts the jugal and ectopterygoid.

Both septomaxillae (figure 2; electronic supplementary material, figure S3 and S5C) are preserved *in situ* but had lost a small medial portion. Each bone is roughly triangular in shape. It is ventrally concave but shallow, to accommodate Jacobson's organ (vomeronasal organ), and its dorsal surface is flattened and smooth, with a prominent process arising close to the anteromedial border of the bone that extends anterolaterally beyond the septomaxillary–maxillary suture. The septomaxilla is extremely complicated in some *Varanus* (for example, *Varanus exanthematicus*) with additional fenestrate laminae and spikes on the dorsal surface. In IVPP V 22770, the medial margin thickens to accommodate a canal for the medial ethmoidal branch of the ophthalmic and ethmoidal nerves (trigeminal nerve branches) and the ethmoidal artery, as in *Lanthanotus* (YPM 6057, digimorph; Evans' Laboratory, CT data of Kanegawa Prefectural Museum of Natural History specimen). This region varies in *Varanus*, from being open dorsally (*Varanus acanthurus*, *V. salvator* and *V. prasinus*), to forming a medial groove (*V. komodoensis* and *V. mokrensis*). The septomaxilla of *V. bengalensis* has a nearly closed canal [39] that extends along the posterior two-thirds of the medial margin, but opens dorsally as a shallow groove further anteriorly. The septomaxilla is supported by the vomer in some *Varanus* species (for example, *V. exanthematicus microsucus*, *V. prasinus* and *V. komodoensis*), but this articulation is not present or preserved in *Archaeovaranus*.

The nasal (figure 2; electronic supplementary material, figure S3 and S5D) is long and unpaired, as in most *Varanus*, *S. ensidens* and *Lanthanotus*, but not *Ovoo* [14] nor *Palaeonecrosaurus* [32]. It is complete except for the posterior tips, but the facet on the frontals shows where the nasal ended. The anterior end appears to bifurcate into separate laminae that diverge slightly to form a narrow dorso-median slot for the tapering nasal process of the premaxilla. However, the laminae are soon fused ventrally to form a shelf that underlies the process posteriorly. The nasal is of consistent width in its anterior three-fifths, but at its contact with the frontals, the nasal widens and then bifurcates. Each of the posterior nasal processes invades the anterior border of the corresponding frontal and extends beyond the posterior margin of the external narial opening. The nasal does not contact either the prefrontal or maxilla, leaving the frontal to form the posterior margin of the external narial opening. In ventral view, a low midline ridge shows the line of fusion of the originally paired nasals. The nasal is relatively long, even by comparison with most living *Varanus* species.

The frontals (figure 2; electronic supplementary material, figures S3 and S5F) are paired, and their medial margins

thicken slightly to form a low dorsal ridge along the median suture. Other than this ridge, also seen in *S. ensidens* [19], and a slightly posteromedial rugosity, the frontal is smooth. As in *Varanus* and *S. ensidens*, the anterior margin of each frontal supports the nasal from below and bears both an anteromedial process and a much longer anterolateral process. The frontals widen slightly from the anterior margin to the level at which their lateral margins enter the orbit. The orbital borders are then parallel for a short distance before expanding at the frontoparietal suture to roughly twice the interorbital width. The cristae cranii (*sensu* [40]) or subolfactory crests are moderately developed but remain well separated in the midline, unlike those of *Varanus*, *Ovoo gurval* [14], and also *Heloderma*, that meet, or nearly meet (for example, the fossil species *V. mokrensis*; [16]), in the midline below the olfactory tracts. Anterior to the orbit in *Archaeovaranus*, the crests gradually reduce in depth and do not contribute to the orbitonasal septum (i.e. the septum is composed only of the prefrontal orbitonasal flange). Further posteriorly, each crest ends abruptly where the frontal starts to expand. Anterolaterally, a large, triangular prefrontal facet invades the crest and extends posteriorly over two-thirds of the frontal length; a much smaller postfrontal facet lies at the posterolateral margin of the frontal. The prefrontal, together with the postfrontal, strongly limits, but does not exclude, the contribution of the frontal to the orbital margin, as in most *Varanus* (except in some old individuals of, for example, *V. komodoensis* and *V. exanthematicus*). The frontoparietal suture is transverse and nearly straight. The structure of this suture is variable in *Varanus*, and it is interdigitating in *V. mokrensis* [16]. Dorsal facets are present on the frontals of *Archaeovaranus*, albeit very small, to support a corresponding anterolateral lappet from the parietal. This tab is commonly present in *Varanus*, and it is weak in *Lanthanotus*. According to Rieppel & Grande [19], *S. ensidens* lacks an anterolateral parietal lappet and the corresponding facet on the frontal.

The parietal (figure 2; electronic supplementary material, figures S3 and S5G) is nearly complete, with only the left postparietal process (supratemporal process) missing. A parietal foramen is present and positioned in the anterior quarter of the parietal table. There is a ridge anterior to the parietal foramen, which is also present, in *S. ensidens* [19] and in some specimens of *Varanus* (for example, *V. prasinus* UF-H-71411). The parietal table is longer than wide and is strongly constricted in its mid-section. It is widest at the frontoparietal suture (nearly twice that of the mid-section) and widens only slightly at the posterior end, before the postparietal processes diverge. The parietal table slightly overhangs the ventrolateral flange (cristae cranii parietalis) in its anterior half, to form a fossa that accommodates the postfrontal facet. There is no alary or epipterygoid process on the flange, but a small posterior surface suggests it may have met the prootic. The postparietal processes are about the same length as the parietal table, and diverge posterolaterally at an angle of around 90°. These processes are lamina-like, with the lamina horizontally oriented at its base but vertically oriented distally at the articulation with the supratemporal. The supratemporal facet extends along with more than half the lateral surface of the postparietal process. The process tapers in its distal quarter, so that the ventral margin of the supratemporal bar is formed by the supratemporal bone which separates the parietal from the squamosal, as in *Varanus*, *Lanthanotus* and also *Heloderma*. However, the supratemporal does not extend on to the medial surface of the postparietal process. At its distal end, the process fails to reach the paroccipital process of the otooccipital, unlike *Lanthanotus*, *Heloderma* and most *Varanus* where there is a small contact. In occipital view, little or no nuchal crest is evident, but there are small, shallow nuchal fossae on each side of the midline. The pit for the ascending process of the supraoccipital (processus ascendens) is located anterior to the posterior margin of the parietal table (invisible in dorsal view) and opens posteriorly.

Seen in dorsal view, the prefrontal (figure 2*a*; electronic supplementary material, figure S3B) is an elongate, strap-like bone, but it is more or less triangular in lateral view. Its anterior lamina is longer than deep and extends more anteriorly than anteroventrally (electronic supplementary material, figure S5E), so contributing more to the roof than the lateral wall of the nasal cavity. This feature is variable in *Varanus*. For example, the prefrontal morphology of *Archaeovaranus* is similar to that of *V. komodoensis*, but differs from that in the deep skull of *V. exanthematicus* where the anterior lamina extends ventrally and contributes only to the lateral wall of the nasal cavity. Anteriorly, a portion of the anterior lamina is overlapped by the facial process of the maxilla. The medial margin of the anterior lamina partially contributes to the margin of the external naris. The orbitonasal flange is broad and its concave ventral margin sutures with the palatine across its width (electronic supplementary material, figure S5E). The medial margin of the flange is vertical and borders the orbitonasal passage. Laterally the prefrontal is sutured to the lacrimal, and together they enclose the more dorsal of the two lacrimal foramina. Dorsally, the tapering posterior frontal process is triangular in section and extends beyond the two-thirds of the frontal. At the level of the orbitonasal flange, it supports the palpebral bone.

Well-developed palpebral bones (figure 2*a*; electronic supplementary material, figure S3B) are preserved on both sides although the posterior tip of the left bone is broken. The broad anterior base attaches to the prefrontal, in the anterodorsal corner of the orbit. The presence of an anterolateral process, as in most *Varanus* species but not, apparently, in *S. ensidens* [19], cannot be confirmed. The posterior process extends straight backwards beyond the midpoint of the orbit. Palpebrals are present, but small, in *Lanthanotus* and absent in *Heloderma*, but they are well developed in the palaeovaranid *P. feisti* [32].

The lacrimal (figure 2*c*; electronic supplementary material, figure S3) is of moderate size. In lateral view, it is triangular and longer than deep, unlike most *Varanus* where the exposed lacrimal is deeper than long [39]. The lacrimal is overlapped by the maxilla and the jugal anteroventrally, and it bears a small posterior projection, as in some species of *Varanus*. As in *Varanus*, there are two lacrimal foramina positioned one above the other. As noted above, the dorsal foramen appears to be enclosed by the lacrimal and prefrontal, whereas the slightly smaller ventral foramen is fully enclosed by the lacrimal itself, the same arrangement as found in *Varanus* and the Late Cretaceous Mongolian *Ovoo* [14]. In all *Varanus* species, the dorsal duct (and therefore its foramen) is larger than the ventral one, but the relative disparity in size of the two foramina varies considerably [39]. In *S. ensidens*, both lacrimal foramina are fully enclosed by the lacrimal [19], but there is disagreement (or variation) about the condition in *Lanthanotus*. Rieppel & Grande [19] wrote that both foramina lie at the prefrontal–lacrimal

border, and the description in McDowell & Bogert [41] implies the same thing. Moreover, this does appear to be the condition in FMNH148589 [42]. However, Norell *et al.* [14] stated that both foramina perforate the lacrimal in *Lanthanotus*, so there may be variation. The lacrimal foramen is single in palaeovaranids [32] and in *Heloderma*.

The right jugal is complete whereas the left one only preserves its anteroventral suborbital ramus (figure 2; electronic supplementary material, figure S3). The bone is long, slender and angulate (figure 2*c*; electronic supplementary material, figures S3E and S6F). The anterior suborbital ramus is relatively deep and bilaterally compressed. Its anterior tip meets the lacrimal and palatine to exclude the maxilla from the orbital margin. Further posteriorly, the jugal articulates with the ectopterygoid medially and ventrally, with the ectopterygoid facet forming a low longitudinal ridge. The lateral surface of the suborbital ramus is smooth and is perforated by a line of three foramina. Posterior to the ectopterygoid articulation, the jugal angles dorsally into a rod-like postorbital ramus. This ramus articulates with the postorbital bone to complete the postorbital bar. The jugal does not contact the postorbitofrontal bone in most *Varanus* and varies in size from a splint-like suborbital element in *V. prasinus*, to a more extensive element that almost contacts the postorbitofrontal in large *Varanus griseus* (BNHM 1974.2418). Although Gilmore [18] could not determine whether the jugal and postorbital met to form a complete bar in his specimen of *S. ensidens* (USNM 2185), and Rieppel & Grande [19] were also unable to reach a firm conclusion on this point, the shape of the jugal in both USNM 2185 and FMNH PR2378 suggests that the postorbital bar was probably completed by the jugal in those specimens.

The postfrontal and the postorbital (figure 2; electronic supplementary material, figure S3B) are separate on both sides of the skull in *Archaeovaranus*. Taken together, the two bones are similar in shape to the (usually) fused postorbitofrontal bone in *Varanus*. Moreover, the shapes of the individual postfrontal and postorbital in IVPP V 22770 are similar to those in a hatchling *Varanus panoptes* [43], where the bones have not yet fused. In dorsal view, the postfrontal (figure 2*a*; electronic supplementary material, figure S3B) appears triradiate, and two medial rami, of about the same length, embrace the lateral margins of the frontoparietal junction. However, linking the two medial rami there is a prominent ventral lamina that supports the frontoparietal suture from below. This lamina is only rarely developed in *Varanus* species such as *V. komodoensis* and is absent in *Lanthanotus*. The anterolateral ramus of the postfrontal is short and extends anteriorly together with the anterior process of the postorbital, almost reaching the jugal. The fourth ramus, a small posterolateral projection that is entirely obscured by the postorbital, supports the postorbital ventrally (electronic supplementary material, figure S6B). The postorbital (figure 2*a*; electronic supplementary material, figure S6C) is an elongate and dorsoventrally depressed element. The bone is robust, being widest just posterior to the articulation with the postfrontal. Anteriorly, the bone narrows into a knob-like anterior process that is inserted between the anterolateral process of the postfrontal and the jugal in dorsal view, completing the postorbital bar. Posteriorly, the bone tapers gradually and articulates with the squamosal from above. It extends posteriorly beyond the midpoint of the supratemporal fenestra.

The postfrontal and postorbital are fused in one articulated skeleton of *S. ensidens* (FMNH PR2378, [19]), but are unfused in the holotype [18]. The two bones are usually fused in adult *Varanus*, but a recent study of skull ontogeny in *V. panoptes* confirmed that the postfrontal and postorbital originate separately during embryonic development and, at least in this species, fuse together very early [43]. However, Mertens recorded finding examples of separate postfrontal and postorbital bones in adults of many species of *Varanus* [2] and considered this to be a variable character without taxonomic significance.

The right squamosal (figure 2*a*; electronic supplementary material, figure S3B) is complete except for its anterior tip, but the shallow squamosal facet on the right postorbital suggests the squamosal almost reached the anterior margin of the supratemporal fenestra, as in *Varanus* and *S. ensidens*, but not *Lanthanotus* or *Heloderma* where the squamosal is reduced. The bone (electronic supplementary material, figure S6E) is dorsoventrally compressed at its articulation with the postorbital anteriorly and mediolaterally compressed where it meets the supratemporal bone posteromedially. The posterior end of the squamosal curves ventrally and terminates as a knob. Together with the supratemporal and the paroccipital process of the braincase, the squamosal suspends the quadrate.

The supratemporal bone (figure 2*c*; electronic supplementary material, figures S3E and S6D) forms a deep and slightly curved lamina. It fits into the facet on the lateral surface of the postparietal process for about half the length of that process. Further posteriorly, the supratemporal wraps under the ventral margin of the postparietal process but does not invade its medial side. At its posterior tip, the supratemporal protrudes beyond the postparietal process and is sandwiched between the paroccipital process and the squamosal.

The left quadrate is preserved between the left pterygoid and squamosal (figure 2*c*; electronic supplementary material, figure S6A); the right quadrate is displaced from the skull and its ventral condyle is missing (figure 1*b*). The dorsal part of the central pillar is curved posteriorly and thus the dorsal condyle faces both dorsally and posteriorly. The posterolateral concha bears a shallow to moderately developed concavity that is bordered laterally by a tympanic crest. The structure of the quadrate is within the range of variation of *Varanus*, although the medial lamina is more developed than in *Varanus*. The dorsal condyle is rounded and suspended by the supratemporal, squamosal and paroccipital process as described above, but there is no obvious notch between the condyle and the tympanic crest. The mandibular condyle is large and saddle-like, with the medial half larger than the lateral half.

The vomers (figure 2*b*; electronic supplementary material, figures S3A and S6G) are elongated and narrow as in *Varanus*. Each has a slightly expanded anterior tip that meets the premaxilla and maxilla, but the anterolateral vomerine margin is notched before expanding into a short flange that met the palatal shelf of the maxilla to enclose the vomeronasal opening (neochoanate palate). In ventral view, the median recess for the palatal sinus is flanked by prominent ventral ridges (electronic supplementary material, figure S6G1). The dorsally open gutter (supravomerine canal in [44]) is wide and deep for almost its entire length, as in *V. salvator*. The gutter is said to be broader and deeper in *S. ensidens* than in *Varanus* [45]. In some *Varanus* (*V. komodoensis*, *V. prasinus* and *V. acanthurus*), the lateral wall of the gutter is much more developed than its medial wall. The two vomers diverge posteriorly to a small

extent, leaving the interpterygoid vacuity extending anteriorly for slightly less than half of the vomer length. This is similar to the condition figured in the Cretaceous *O. gurval* [14]. The vomers in *Saniwa* are in contact medially throughout most of their length [45], but variable degrees of divergence are seen in *Varanus*, *Lanthanotus* and *Heloderma*. Posteriorly, the vomer meets the slender anterior process of the palatine in a loose, slot-like joint. One short process passes ventral to the anterior tip of the palatine and one much longer process lies dorsal to the palatine and extends more than halfway across the anterior vomerine ramus of the palatine.

The palatine (figure 2*b*; electronic supplementary material, figure S6H) is short and triradiate with little or no choanal fossa. There seem to have been two rows of palatine teeth, as evidenced by two edentulous ridges (electronic supplementary material, figure S4B), with one remnant tooth on the right palatine and highly dense tooth-like structures on the CT slices where the palatine teeth should have been. The anterior vomerine ramus is bar-like and articulates with the vomer as described above. The lateral maxillary ramus is greatly expanded, to a greater degree anteriorly than posteriorly, and has a long lateral suture with the maxilla. This ramus also meets the ectopterygoid at its posterior tip to exclude the maxilla from the margin of the suborbital fenestra. A large superior alveolar canal is clearly present (electronic supplementary material, figure S6H), as in all *Varanus*. The posterior pterygoid ramus is broader but shorter than the anterior vomerine ramus, turning ventrally to articulate with the pterygoid in an interlocking joint. Dorsally, at the junction of the vomerine and maxillary rami, the palatine bears a ridge that meets the orbitonasal flange of the prefrontal.

The pterygoid (figure 2*b*; electronic supplementary material, figure S6J) is triradiate with a broad Y-shaped palatal plate and a long, slender posterior quadrate process. There are two rows of teeth along with the raised medial border of the palatal plate and these extend onto the anterior palatine process. The pterygoid flange extends anteroventrally and bears an articulation facet for the ectopterygoid medially and dorsally. Ventral to the concavity for the basipterygoid process, just posterior to the palatal plate, there is a well-developed medially extending shelf. The quadrate process is roughly triangular in section for half of its length and then becomes laminar with a longitudinal shallow groove along with the medial surface. Its posterior end is pointed and would have articulated with the quadrate in a loose joint. In dorsal view, at the level of the basipterygoid joint, the deep fossa columellae for the articulation of the epipterygoid is visible.

The ectopterygoid (figure 2*b*; electronic supplementary material, figures S3A and S6I) runs roughly anteroposteriorly. It is weakly curved and twisted at the midpoint. Anteriorly the ectopterygoid articulates with the maxilla and the palatine as in *Varanus*, *Lanthanotus*, *Heloderma*, *Ovoo* [14] and *Saniwa* [19], and with the jugal dorsally. The posterior end diverges into dorsal and ventral processes that clasp the pterygoid from the medial and dorsal sides.

The epipterygoid (figure 2; electronic supplementary material, figure S3) is a rod-like element, as in all lizards, with both ends slightly expanded. The right one is preserved *in situ*, fitting into the fossa columellae of the pterygoid ventrally and articulating with prootic dorsally. The left epipterygoid is disarticulated and displaced below the parietal. The orientation of the epipterygoid can be considered as vertical at rest.

There is no sign of an orbitosphenoid in the CT slices, but we cannot be sure whether or not an ossified element was present owing to the slight disarticulation in this region.

The braincase (supraoccipital, basisphenoid with parasphenoid, basioccipital, prootic, otooccipital) was well preserved except that the left paroccipital process of the otooccipital is missing. The braincase is exposed in dorsal, ventral and occipital views in the specimen (figure 2; electronic supplementary material, figure S3), and the anatomical observations are supplemented by the CT scan data. The CT scan shows that existing cavities in the braincase (such as the otic capsule) contain crystals that blur neighbouring structures owing to their strong reflective properties. As a result, the sutures between elements, especially those parts within the matrix, are difficult to discern and the braincase has been segmented as a single structure (figure 2*d*,*e*; electronic supplementary material, figure S7). The presence of foramina has been checked on both sides, as well as on the original scan slices for confirmation. The braincase contacts the parietal via (i) the ossified ascending process of the supraoccipital and (ii) the anterodorsal tips of the alar processes of the prootics. There are no additional contacts lateral to the midline between the supraoccipital and the parietal. No stapes is preserved *in situ*, nor identified within the block.

The braincase floor, as a whole, is elongate (electronic supplementary material, figures S3A and S7A). The basioccipital is roughly rectangular in ventral view and narrows abruptly into a small, rounded occipital condyle. In ventral view, the basisphenoid-basioccipital suture (figure 2*b*; electronic supplementary material, figure S7A) is an inverted V-shape with a flat vertex, terminating laterally at the apices of the basal tubera. Norell & Gao [46] described the basisphenoid and basioccipital suture in *Estesia mongoliensis* as strongly arched anteriorly, which is very similar to the 'obtusely angulate suture' noted by McDowell & Bogert [41] in basal anguimorphs, and also present in *Heloderma*, but different from the straight-line suture in *Varanus* and *Lanthanotus*. This suggests that *Archaeovaranus* retained the primitive state. The basal tubera are well developed, although the epicondyles are not preserved, and they are positioned posterolaterally, with their basioccipital apex just behind the base of the prootic-opisthotic suture (figure 2*e*). In *Lanthanotus* and *Varanus*, the basal tubera are positioned anteromedial to the prootic-opisthotic suture, with their apices at the lateral junction of the sphenoid and basioccipital; they lie further posteriorly in *Heloderma*. As in some *Varanus* species (e.g. *V. griseus*), the tubera of *Archaeovaranus* extend both laterally and ventrally, such that the crista tuberalis slopes dorsally. However, in other *Varanus* species (e.g. *V. salvator*), the tubera just extend laterally and the crista tuberalis is almost horizontally positioned. The dorsal surface of the crista tuberalis is excavated by the occipital recess.

The sphenoid (figure 2*d*; electronic supplementary material, figure S7A) is a composite of the basisphenoid and dermal parasphenoid. The parasphenoid is firmly fused to the basisphenoid, leaving no trace of the suture between them. The sphenoid (figure 2*b*; electronic supplementary material, figure S7A) is narrowest just posterior to the basipterygoid processes, but then expands to form a pair of prominent processes that diverge postero-ventrally to reach the basal tubera (see above). Anteriorly, the basisphenoid bears a pair of robust basipterygoid processes which are short but greatly expanded distally. The medial margin of each process is

deflected dorsally and forms a dorsally upturned projection that would have increased the articular surface for the pterygoid. The two basipterygoid processes diverge at an acute angle (about 60 degrees) and the bases of trabeculae cranii are located between them, supported from below by an ossified parasphenoid rostrum. The parasphenoid rostrum is slender and extends anteriorly well beyond the anterior termination of the basipterygoid processes. Dorsal to the bases of the two trabeculae cranii (figure 2*d*) lies the hypophysial fossa into which the internal carotid foramina open. The two foramina are positioned close to each other and to the braincase floor. Lying between the base of each trabeculum and the corresponding basipterygoid process is the anterior opening of the vidian canal which is almost aligned with the internal carotid foramen. The foramina for the abducens nerves (CN6) are located further dorsally on the dorsum sellae, dorsolateral to the anterior openings of the vidian canal. The abducens foramina are also visible in dorsal view. The dorsum sellae is deep and the alar process of the sphenoid is well developed, giving the crista sellaris a concave dorsal margin. The alar process protrudes anteriorly and downwards, and together with the anterior inferior process of the prootic, partially encloses the notch (incisura prootica) for the trigeminal nerve. Laterally the entry foramen for the vidian canal lies just posterior to the base of the basipterygoid process, and well below the prootic-basisphenoid suture (figure 2*e*) as in *Lanthanotus* and most *Varanus* (such as *V. salvator*), although in *V. exanthematicus*, the posterior opening of the vidian canal is located closer to the prootic-basisphenoid suture. In *Heloderma*, the entry foramen is further posteriorly positioned.

The supraoccipital (electronic supplementary material, figures S7B and S7C) is well preserved and is nearly completely exposed in dorsal view. There is a low sagittal ridge on the dorsal surface that is continuous anteriorly with the ascending process. Evans [38] described the supraoccipital in *Varanus* as having a steeply inclined posterodorsal surface with a variably developed median crest, but this is not always the case in *Varanus*. Anteriorly the ascending process inserts into a posteriorly opening pit in the parietal. The posterior margin of the supraoccipital, forming the dorsal margin of the foramen magnum, is gently curved as in most *Varanus* and *Shinisaurus* (but angulated in *Lanthanotus*). In *S. ensidens*, it is described as angulated [19] but, based on their figure, the angulation is not prominent and could be an artefact of preservation. The cranial opening of the endolymphatic duct is not discernible on the CT model owing to the presence of crystals in that area.

The lateral wall of the ossified braincase (figure 2*e*) is mainly made up of the prootic and the otooccipital which enclose the rounded fenestra ovalis. The fenestra lies immediately above the dorsoventrally elongate lateral opening of the recessus scalae tympani in the otooccipital. The two openings are separate by a well-developed crista ventrolateralis that is horizontally positioned. A long posterior process of the prootic extends onto the otooccipital, but its extremity is well separated from the posterolateral end of the paroccipital process. The prootic bears a moderately developed prootic crest and an undivided facial foramen lying just below the prootic crest, posterior to the base of the alar process of the prootic. The division of the facial foramen is variable in *Varanus* [47]. A divided facial foramen was reported for *L. borneensis* [5,48], but an undivided foramen was observed in the CT scan of the Kanagawa Museum specimen. The condition is not known for *Saniwa*. The anterodorsal alar process of the prootic is well developed as a subrectangular projection. At its tip, it meets the weakly developed lateral descending flange of the parietal, and laterally, it supports the dorsal head of the epipterygoid. The anterior inferior process is smaller than the alar process of the sphenoid and, together with the anterodorsal alar process, forms the trigeminal notch. In medial view, there seems to be a low medial ridge at the base of the prootic alar process, but there is no supratrigeminal process. The presence of a medial ridge and/or a supratrigeminal process is variable in *Varanus*. A faint ridge is present in *V. exanthematicus* (FMNH-58299, digimorph), but was absent in other *Varanus* studied herein (*V. salvator*, *V. komodoensis*, *V. acanthurus* and *V. prasinus*). The medial acoustic recess contains the internal facial foramen and foramina for the vestibulocochlear nerve.

The paroccipital process of the otooccipital in *Archaeovaranus* is well developed and extends posterolaterally. Its length and orientation are variable in *Varanus*, ranging from a long, posteriorly oriented process in *V. komodoensis* to the short, nearly laterally directed one in *V. salvator*. In *Archaeovaranus*, the ventral margin of the paroccipital process continues ventrally towards the basal tubera and, together with the exoccipital, forms the occipital surface of the braincase (electronic supplementary material, figure S7C). In occipital view, this ventrolateral margin of the otooccipital is deeply notched to form a prominent ventral process (black arrow in electronic supplementary material, figure S7C), a condition that differs from that in *Varanus*. A large vagus foramen opens onto the occipital surface lateral to the foramen magnum. Two hypoglossal foramina perforate the exoccipital internally and exit via the vagal canal, a condition similar to that in *Saniwa* [19]. There is only one internal hypoglossal foramen in *Lanthanotus*, and it does not exit via the vagal canal, but opens on the medial margin of the vagus foramen. The condition in *Varanus* may be variable as both one and two internal foramina have been reported [38]. The vagus foramen lies further ventrally in *Varanus* and *Lanthanotus* than in *Archaeovaranus*, being below the level of the dorsal margin of the exoccipital condyle.

The occipital condyle (electronic supplementary material, figure S7C) is composed of the basioccipital and exoccipitals, with the basioccipital making a slightly larger contribution. The exoccipitals do not meet to exclude the basioccipital from the dorsal margin of the occipital condyle.

As in *Varanus* and *Lanthanotus*, but not *Heloderma*, the lower jaw (figure 1*a*; electronic supplementary material, figure S4A) of *Archaeovaranus* is characterized by a reduced articulation between the anterior dentary unit (dentary, splenial and coronoid) and the posterior articular unit (surangular, prearticular and articular). No angular was observed. This intramandibular articulation is visible in the right mandible but is also evidenced by the fact that the articular unit of the left lower jaw has separated from the dentary unit.

The dentary, forming roughly half the length of the mandible, is slender and tapers anteriorly (electronic supplementary material, figure S4A). Its lateral surface is perforated by a line of at least six neurovascular foramina. Posteriorly the dentary seems to bifurcate, if the posterior notch is natural. The subdental shelf is broad but there is no subdental ridge. The meckelian fossa is open ventrally along with its anterior half but is covered posteromedially by the

splenial and coronoid. The intramandiblar septum is probably obscured by the coronoid and the prearticular in the medially exposed right mandible.

The left splenial is exposed in internal view and may be complete, but it is obscured by the dentary except along with the ventral margin (electronic supplementary material, figure S4A). Adjacent to the right lower jaw is a thin lamina of bone that might, by its length, be the right splenial. The splenial extends anteriorly beyond the midpoint of the dentary. By the impression on the inner surface of the preserved right lower jaw, the posterior extremity of the splenial did not extend beyond the dorsal prominence of the coronoid. No other detail is visible.

The coronoid (electronic supplementary material, figure S4A) is long and low. The anterior process runs along with the dorsal margin of the surangular to clasp the coronoid process of the dentary between medial and lateral laminae, as in *Varanus* and *S. ensidens*, but also *Heloderma*. The medial lamina is expanded (electronic supplementary material, figure S4A) and extends forward to enclose the anterior mylohyoid foramen together with the splenial, as in *Varanus*, *Lanthanotus* and *Heloderma*. A low ridge originating from the ventral margin of the lateral lamina extends posterodorsally towards the dorsal prominence of the coronoid bone, creating a posterior depression for attachment of the adductor mandibulae externus superficialis [40]. A posteromedial process is preserved on the right lower jaw, partially obscured by a rib fragment. It extends ventrally and posteriorly, possibly forming the anterior margin of the adductor fossa.

The right and left postdentary (articular) units (electronic supplementary material, figures S4A and S4D) are both preserved in medial view, but the region of the adductor fossa is missing from the left lower jaw. On the right mandible, the adductor fossa is small, enclosed by the surangular dorsally and the prearticular ventrally. The surangular extends anteriorly to reach the coronoid anteromedial process. The dorsal margin of the surangular becomes thicker posteriorly. The prearticular is fused with the articular and is long enough to exceed the level of the anterior tip of the coronoid as preserved. The prearticular is wider than the surangular in medial view anterior to the adductor fossa and bears no angular process. The retroarticular process is preserved on the left side (electronic supplementary material, figure S4D). It widens posteriorly to become subrectangular but is slightly medially deflected. A shallow retroarticular fossa appears to have been present.

The marginal dentition, including the premaxillary, maxillary and dentary teeth, is characterized by the presence of plicidentine (electronic supplementary material, figure S4C), as in *Varanus* and *S. ensidens*, but also *Heloderma* and possibly *Ovoo* [14]. The teeth are highly pleurodont and expanded strongly at the base (i.e. extensive attachment with the jaw bone). The tooth crowns are pointed, recurved and probably compressed mediolaterally, but it is difficult to assess how strong the compression is. No groove or ridge (cutting edges) is discernible along with the anterior or posterior tooth margins. The teeth are well spaced, small anteriorly and becoming larger posteriorly. Many replacement teeth are preserved, and represent at least two generations. The tooth number is uncertain, but the estimated maximum of 10 maxillary teeth is based on the distribution of the preserved teeth on both the left and right maxilla, whereas tooth counts for premaxillary and dentary are estimated at about eight and 11, respectively. The palatal teeth are arranged in roughly two rows on the pterygoid and are present on palatine, again possibly in two rows (electronic supplementary material, figure S4B). They are small simple bulging structures. Palatal teeth are absent in *Varanus* and *Heloderma*, but are present in *Lanthanotus* (single row on pterygoid, variably on palatine, [41]), *Ovoo* (single palatine row, two pterygoid rows, [14]) and *S. ensidens* (single continuous row on palatine and pterygoid, [18]).

No hyoid elements were identified across the whole block.

(b) Vertebral column

The specimen preserves 20 procoelous presacrals (including the axis and at least two further cervicals), two sacrals, 11 disarticulated caudals and a further series of articulated caudals. Accurate counts of the cervical, trunk and caudal vertebrae are not possible. The presacral count in *Varanus* ranges from 27 to 35, with most species having 28–29 [49], and there are 31 presacrals in *S. ensidens* [19], 34 in *Heloderma* and 36 in *Lanthanotus* [41].

The elements of the atlas have not been identified, but the axis (figure 1*b*; electronic supplementary material, figure S8F) lies beside the left femur and is almost complete. It is exposed in right lateral view, but the right prezygapophysis and the right half of the condyle are missing. The neural spine is anteroposteriorly expanded, and a hypapophysis (and the corresponding intercentrum) is present. The neural spine extends slightly beyond the posterior termination of the condyle but does not reach that of the hypapophyses. The synapophysis is broken and therefore its orientation is unknown. A second intercentrum appears to be present *in situ*, partially fused with the axis. There are another two cervical vertebrae preserved (judging by the presence of hypapophyses), one near the skull (electronic supplementary material, figure S2) and the other above the tibia (electronic supplementary material, figures S2 and S8G). The former is preserved in left lateral view with the neural spine broken away, and the second seems to be associated with a separated epiphysis. It is difficult to tell whether the distal tips of the hypapophyses widen laterally but they are clearly enlarged, as evidenced by the one above the left tibia.

The trunk (dorsal) vertebrae are mostly exposed in ventral view, showing a clear precondylar constriction (figure 1*b*; electronic supplementary material, figure S8E). Some other vertebrae, preserved in lateral or dorsal view, show a complete or nearly complete neural spine. Where preserved, the synapophyses are massive, dorsoventrally elongated and located just below the prezygapophysial process (electronic supplementary material, figure S8B). The vertebral condyle is compressed and faces dorsally and posteriorly, and the neural spine bears a horizontal dorsal margin that is slightly thickened posteriorly (electronic supplementary material, figures S8A and S8B), as in *Varanus*, *Lanthanotus* [50] and *S. ensidens*. The anterior margin of the neural spine varies in its orientation along with the presacral series from posterodorsally inclined to vertical (figure 1*b*), and neural spine height probably also varies. Striations are evident on the neural arch (electronic supplementary material, figure S8A) (fibrous striae in [51]). Smith *et al.* [20] suggested that vertebral striae might have arisen on the *Varanus* stem and have been retained as a plesiomorphy in many crown

Varanus, especially the African species. These striae are also obvious on the trunk vertebrae of *S. ensidens* supporting the suggestion of Smith *et al.* [20] that this feature was already present by the Eocene.

One trunk vertebra (electronic supplementary material, figure S2, trV-a), lying adjacent to the right lower jaw, has a neural spine only slightly longer than tall (i.e. it is an anterior trunk vertebra) and the anterior margin of the spine is posterodorsally inclined. On the two trunk vertebrae which were removed from the main postcranial mass, the neural spines are rectangular in shape with a vertical anterior margin and are much longer than tall (ratio is about 2 : 1), suggesting they are middle or middle-posterior trunk vertebrae (electronic supplementary material, figure S8B). Accessory articulations are present between successive neural arches (electronic supplementary material, figure S8C and S8D) and correspond to Hoffstetter's [52] definition of a pseudozygosphene in having an anterior lamina that underlaps the posterior margin of the neural arch of the preceding vertebra [52]. The pseudozygantrum, if treated as an accessory articulation, is evidently present in IVPP V 22770. Rieppel & Grande [19] followed Hoffstetter [52] and regarded a pseudozygosphene as present variably in *S. ensidens*, but it might be non-articular as a pseudozygantrum is absent. A pseudozygosphene is also present in some *Varanus*, but seems to be a non-homologous structure on the anterior margin of the neural arch [5]. Hoffstetter [52] suggested that the pseudozygosphene is for the attachment of intervertebral muscles, but the presence of both pseudozygosphene and pseudozygantrum in *Archaeovaranus* vertebra argues against this hypothesis. Therefore, the presence or absence of the pseudozygosphene should be treated with caution when comparing different species from the literature.

Both sacral vertebrae (electronic supplementary material, figure S8H) are preserved in ventral view and are in articulation. Their centra are shorter than those of the presacrals. The transverse processes of the first sacral are robust and that of the second is slender (left side only complete).

Two caudal vertebrae (figure 1*b*) are preserved near the sacrals and, based on their morphology, they are probably anterior caudals but not pygals as pedicels for haemapophyses are present on both, placed just anteroventral to the condylar articulation. The pleurapophyses are preserved but are not complete on either side. Several disarticulated caudals with tall neural spines and haemal arch pedicles (e.g. those in the electronic supplementary material, figure S8G and S8I) are scattered on the block, from close to the skull to the middle of the postcranial mass. The posterior tail is linear with the vertebrae in articulation (figure 1*b*, tail; electronic supplementary material, figure S8J). There are no autotomy fracture planes visible in any preserved caudals.

The ribs are not associated with the vertebrae and show a generally similar morphology with an anteroposteriorly elongated articular head.

(c) Pectoral girdle and forelimbs

The left scapula and coracoid are exposed in lateral view (figure 1*b*; electronic supplementary material, figure S9A). The two bones are detached from each other, but are in roughly anatomical positions. The scapula and the coracoid contribute equally to the glenoid. Based on the position of the supracoracoid foramen, there is a single coracoid emargination, and the plate-like shape of the bone ventral (anatomically) to this emargination is similar to that in *S. ensidens* [18]. This morphology distinguishes these taxa from both *Varanus* and *Lanthanotus* [50] where there are two coracoid emarginations, and from *Heloderma* where there are none. The spike-like process remaining above the coracoid emargination sutures to the scapula and contributes to the border of the scapulocoracoid emargination. As preserved, the scapula is broad and, as in *Varanus* and *Lanthanotus*, there seems to be no scapular emargination.

Both humeri (figure 1*b*; electronic supplementary material, figure S9B) are preserved. They are robustly built and show little torsion. The left humerus is completely exposed in dorsal view, but only the proximal half of the right bone is visible. The proximal epiphysis is ossified and completely fused with the humerus, but the distal epicondylar epiphyses are missing on both sides. Both ends of the humerus are greatly expanded. The proximal humeral condyle, medial tuberosity and lateral tuberosity are distinct. A deltopectoral crest is present, but its size is difficult to assess. The distal end of the bone bears a broken posterior (anatomical) margin that suggests the presence of an ectepicondylar foramen. Overall, the configuration of the humerus is similar to that of *Varanus* (for example, *V. salvator*) and more robust than that of *Lanthanotus* [50].

Neither radius is preserved. The right ulna (preserved with the skull mass) (figure 1*a*, ul; electronic supplementary material, figure S9C) bears a prominent olecranon process and a deep posterior fossa like that in some *Varanus*.

(d) Pelvis and hindlimb

No pelvic elements have been identified.

Both femora are preserved (figure 1*b*; electronic supplementary material, figure S9D) and are similar in length to the humeri (removing the distal epicondyles of both). The right femur is complete in dorsal view and the left one is exposed only at the distal end. The proximal femoral condylar epiphysis is present and fused with the shaft, but the internal trochanter is buried in the matrix. The distal epicondyle is missing, suggesting that it had not fused with the femoral shaft.

Both tibiae and fibulae are preserved (figure 1*b*; electronic supplementary material, figures S9E and S9F). The proximal part of the right tibia and the distal part of the left one are located posterior to the right femur. Both the fibulae are preserved without epiphyses. Further details are difficult to discern.

As preserved, the right astragalus is separate from the calcaneus, as in *S. ensidens* (FMNH PR 2378). The fusion of the astragalus and calcaneus occurs very late during development in at least some *Varanus* (see discussion below on the ontogenetic stage of IVPP V 22770). The astragalus (figure 1*b*; electronic supplementary material, figure S9G) is compressed and plate-like, exposing the tibial facet and half of the fibular facet. The two facets are separated by a prominent notch as in *Varanus*. The distal margin, although incomplete, displays a concavity for articulation with the fourth distal tarsal. The antero-distal border of the bone is slightly thickened as in *Varanus*.

Some metacarpals / metatarsals and phalanges (figure 1*b*; electronic supplementary material, figure S9H) are preserved

in situ and partially articulated, but their detailed morphology is difficult to determine.

6. Results and discussions

(a) The phylogenetic position of *Archaeovaranus lii*

As outlined in the Material and Methods section (and also in more detail in the electronic supplementary material, text S3), two analyses were run using the data matrix of Gauthier *et al*. [7], with or without a molecular constraint, and then eight different phylogenetic analyses were run using the matrix of Villa *et al*. [17], with different outgroup taxa (*Shinisaurus* or *Heloderma*) and with a subset of marine dolichosaurs included or excluded. Using the Gauthier *et al*. [7] matrix, the first (unconstrained) analysis found 12 most parsimonious trees (MPTs) with a tree length of 5326 steps while the second (constrained) analysis produced 1680 MPTs with a length of 5481 steps. Both analyses recovered *Ar. lii* within Anguimorpha. The strict consensus tree of the unconstrained analysis positioned *Ar. lii*, together with *Aiolosaurus oriens* (Late Cretaceous, Gobi Desert), on the stem of a clade comprising *Lanthanotus*, *Saniwa* and *Varanus* (electronic supplementary material, figure S11), whereas the strict consensus of the constrained analysis placed *Ar. lii* as the sister taxon of *Varanus* (electronic supplementary material, figure S12).

Using the Villa *et al*. [17] matrix, the choice of the outgroup did not affect the tree length, MPTs or the topology of the strict consensus trees (electronic supplementary material, figures S13–S24). Whether dolichosaurs are included or not does not influence the ingroup relationships of the genus *Varanus* in the combined analyses but their inclusion did affect the placement of *Paranecrosaurus* and *Eosaniwa* in the morphology only analyses. Moreover, the placement of dolichoaurs themselves also differed between the analyses depending on whether combined evidence or morphological characters alone were used. This reflects the lack of consensus between other researchers (e.g. [7,31,53,54]). Nonetheless, the positions of the other taxa were relatively stable across all the analyses. The combined analyses recovered some of the known clades within *Varanus*, such as the *gouldii* group (part of the *Varanus* subgenus) and the *Odatria* subgenus of the Indo-Australian clade, and the two Indo-Asian clades, but the other *Varanus* species collapsed probably owing to poorly preserved fossil taxa such as *Varanus cf. bengalensis*.

Saniwa ensidens had long been regarded as the closest relative of *Varanus* based on morphological comparison (e.g. [18,41]), morphological character analyses (e.g. [55,56]) and combined analyses with an extensive molecular dataset (e.g. [10,17]). However, each of the analyses using the matrix of Villa *et al*. [17] and the constrained analysis of the Gauthier *et al*. [7] matrix herein, all placed *Archaeovaranus* as the sister taxon of *Varanus*, with *S. ensidens* as the sister taxon to these two. Figure 3 shows the strict consensus (136 MPTs, tree length 10700, consistency index 0.311, retention index 0.451) of an analysis using the Villa *et al*. [17] combined evidence matrix, with *Heloderma* as the designated outgroup, and dolichosaur taxa de-activated.

Stem-ward of the *Saniwa* + (*Archaeovaranus* + *Varanus*) clade there is a succession of varaniforms from the Late Cretaceous of Mongolia including *Telmasaurus grangeri* [11], *Saniwides mongoliensis* [12], *Ai. oriens* [13] and *O. gurvel* [14], with the lanthanotids (*Lanthanotus* and the Late Cretaceous Mongolian *Cherminotus*) as sister to those (figure 3; electronic supplementary material, figures S13–S24). The European Palaeogene palaeovaranids (*sensu* [57]) *Ophisauriscus* (*Necrosaurus*) *eucarinatus* and *Paleovaranus* (*Necrosaurus*) *cayluxi* were positioned on the stem of the *Lanthanotus* + *Varanus* clade, but not as sister taxa, and the positions of *Paranecrosaurus (Saniwa) feisti* [32] and *Eosaniwa kuhni* clade varied depending on the inclusion or exclusion of dolichosaurs, and the use of morphological or combined evidence. This contrasts with the findings of Smith & Habersetzer [32] who found a palaeovaranid clade as the sister group of Lanthanotidae + Varanidae.

(b) Comparison with other fossil and extant varanid relatives

Although phylogenetic analyses using morphological characters usually place *Heloderma* and its fossil relatives as the sister group of *Varanus* + *Lanthanotus* (e.g. [7,37]), analyses incorporating molecular data generally place *Heloderma* closer to anguids (e.g. [9,33,53,58]) than to varanids (i.e. they are not varaniforms). This means that several characters occurring in both Varanidae and Helodermatidae (e.g. plicidentine, a short maxilla, well-spaced recurved teeth, an elongated anterior coronoid process, narrow vomers, cristae cranii of the frontals meeting in the midline under the olfactory tracts, and a posteriorly extended external narial opening) arose at least twice, probably owing to the predatory habits of these lizards [32]. These common characters complicate comparisons with fossil taxa, especially when the representative specimens are incomplete. Nonetheless, *Heloderma* differs from both *Varanus* and *Lanthanotus* in having a single lacrimal foramen and paired nasals (contra two lacrimal foramina and fused nasals), in having thick tubercular osteoderms, and in lacking a palpebral and an intramandibular joint.

Designated palaeovaranids (*sensu* [32,57]) including *Ophisauriscus*, *Palaeovaranus* and *Paranecrosaurus* differ from lanthanotids and total group varanids in having a single lacrimal foramen, a more limited external narial extension and in lacking a functional intramandibular joint [32]. However, in our analyses, these taxa did not form a monophyletic group.

Total group Varanidae (stem + crown) differs from known lanthanotids in several characters including longer and narrower nasals and an elongated anterior process of the coronoid that clasps the dentary. Other characters like nasal fusion (*Ai. oriens*, [13]; some *Varanus*, [2]), the presence of plicidentine (unknown in *Aiolosaurus*) and the position of the dorsal lacrimal foramen (within lacrimal or at prefrontal-frontal margin) are unevenly distributed within the stem-varanid group. This distribution could reflect instability in this part of the tree, but also that these characters are labile, as evidenced by the morphology of *Heloderma*.

Archaeovaranus lii and *S. ensidens* differ from the Late Cretaceous stem-varanids and resemble *Varanus* in the posterior extension of the external narial openings to reach the frontals, the fusion of the nasals into a narrow midline bar and the presence of an intramandibular joint. The skull roof in *Archaeovaranus* looks similar to that in *S. ensidens* (i.e. extended

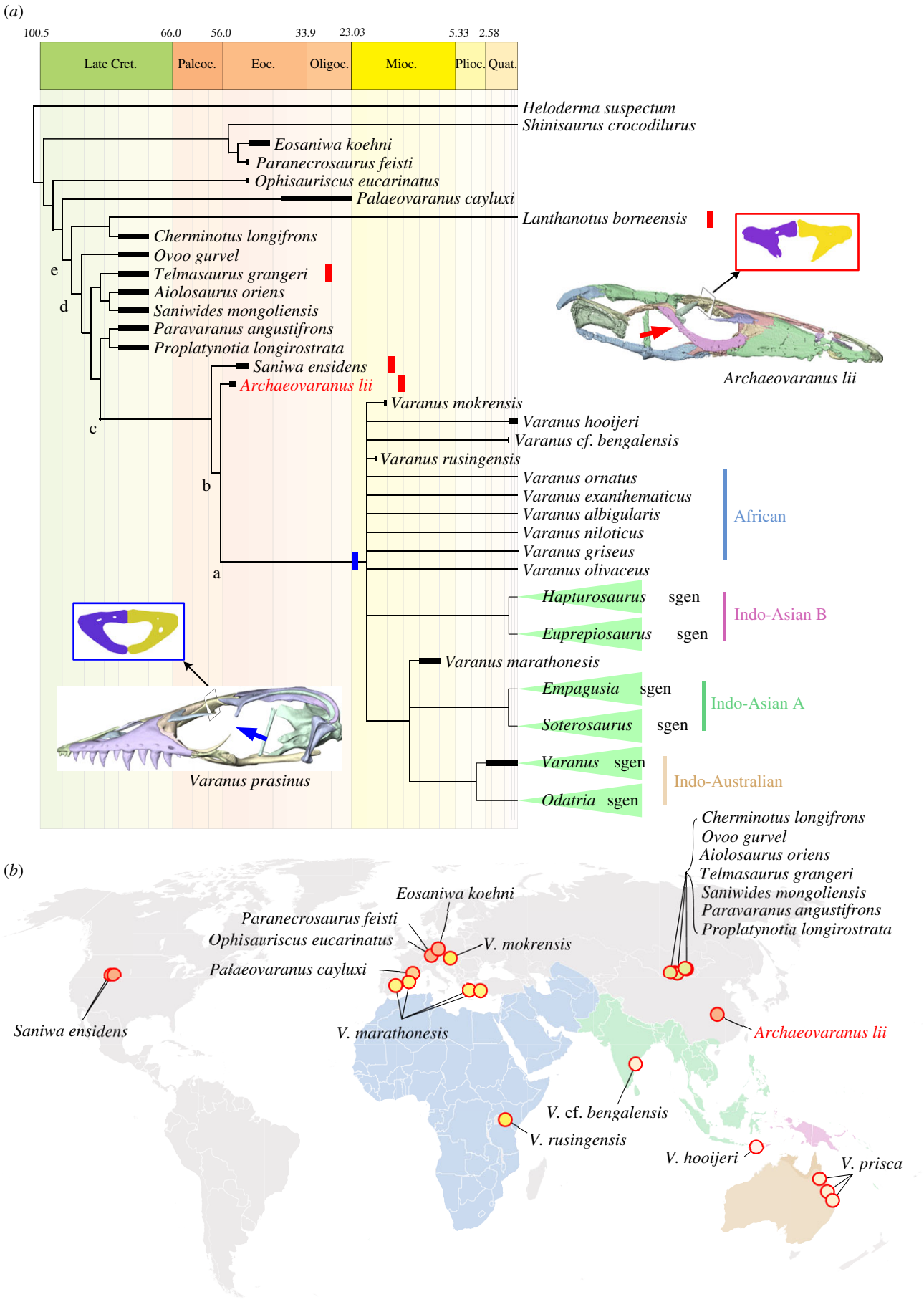

Figure 3. (*Caption overleaf.*)

external narial openings, unpaired nasal, paired frontals), except that the snout is longer and the frontal is relatively shorter in *Archaeovaranus*. In the palate, there are two continuous rows of teeth on palatine and pterygoid in *Archaeovaranus*, but only one row in *Saniwa* [18]. There are two internal hypoglossal foramina in *Archaeovaranus*, but

Figure 3. (*Overleaf*.) (*a*) Time-scaled phylogeny of Varanidae and its living and fossil relatives. The tree is a simplified version of the strict consensus tree (electronic supplementary material, figure S23) derived from the analysis based on Villa *et al*.'s [17] combined matrix. See the electronic supplementary material, text S3 for the detailed settings. The subgenera *Empagusia*, *Euprepiosaurus*, *Hapturosaurus*, *Odatria, Soterosaurus*, *Varanus* follow Auliya & Koch [1] and Brennan *et al*. [10]. The geographical distributions of the different clades of living *Varanus* refer to Pianka *et al*. [4]: the Indo-Australian clade is distributed in the yellow and purple regions, whereas the Indo-Asian B clade in the purple region and the darker yellow region of Australia; the African and Indo-Asian A clades are in the blue and green regions, respectively. The skull of *Varanus prasinus* displays an enclosed bony frontal olfactory canal (transverse section within inset square) and the incomplete bony postorbital bar (blue arrow), whereas the skull of *Archaeovaranus lii* displays the open frontal olfactory canal (transverse section within inset square) and the complete bony postorbital bar (red arrow), conditions also present in other stem-varanids such as *Saniwa ensidens* and *Telmasaurus grangeri*, as well as the living *Lanthanotus*. The synapomorphies supporting the nodes, labelled as a, b, c, d, e, are listed in the electronic supplementary material, text S4. (*b*) Geographical distribution of the fossil varanid relatives, with the colours of the dots representing the temporal distribution of each taxon (corresponding to the colours used on the time chart in (*a*)).

only one in *Saniwa* [19] and *Lanthanotus*. The condition in *Varanus*, however, may be variable with one or two internal foramina [38].

Archaeovaranus resembles *Varanus* and differs from *Saniwa* in several features that support its sister group relationship (see the electronic supplementary material, text S4). These include having a slightly shorter maxillary tooth row (one tooth extends below the orbit in *Archaeovaranus* versus two to three in *Saniwa*) and a premaxilla with a posteriorly tapering nasal process (the tip of the process in *Saniwa* is slightly expanded and bifurcated rather than tapered [19]). A small parietal tab is present on the frontal in *Archaeovaranus*, resembling the condition in *Varanus*, but not *Saniwa* [19]. As in *Varanus*, the dorsal lacrimal foramen of *Archaeovaranus* is enclosed by the prefrontal and the lacrimal, whereas both lacrimal foramina are fully enclosed by the lacrimal in *Saniwa* [19].

Despite the similarities, *Archaeovaranus* differs from *Varanus* in several characters, where it shows the primitive state. In *Archaeovaranus*, the cristae cranii of the frontals are completely separate from each other whereas they meet or nearly meet in the midline in *Varanus*; the bony postorbital bar is completed by the jugal in *Archaeovaranus* but it is incomplete owing to the loss of the jugal-postorbital articulation in *Varanus*; there are both palatine and pterygoid teeth in *Archaeovaranus*, but none in *Varanus*. The otooccipital in *Archaeovaranus* has a deep notch lateral to the vagus foramen in occipital view, but the notch is absent or very shallow in *Varanus*. The basisphenoid-basioccipital suture in *Archaeovaranus* is inverted V-shaped with a flat vertex, but transverse in *Varanus*. In *Archaeovaranus*, the scapula is unemarginated, there is a scapulocoracoid emargination, and the coracoid has a single emargination, but in *Varanus* and *Lanthanotus*, the coracoid has two emarginations.

(c) The size and ecology of *Archaeovaranus lii*

To estimate the TL of the long bones in *Archaeovaranus* holotype (IVPP V 22770), we measured the length of these bones with and without epiphyses in the specimen (electronic supplementary material, table S4) and *Varanus* specimens from the NHM London (electronic supplementary material, tables S5–S8). We then ran regressions of these to calculate an estimated total femur length (i.e. including the epiphyses) of 43.48 mm for the holotype specimen of *Archaeovaranus* and a total humerus length of 43.04 mm. The estimated total ulna and fibula lengths were 29.84 mm and 31.94 mm, respectively. However, note that the estimate of total ulna length for the *Ar. lii* holotype, as calculated using the regression of the NHM dataset, was less (at 29.84 mm) than the actual measured length of the ulna as preserved (31.47 mm), with the proximal (olecranon) but not distal epiphysis. For this reason, the actual measured length of the ulna was used in the calculations of total limb length. This represents a slight underestimate of the ulna length in life, but as the distal ulna epiphysis in *Varanus* is less than half the size of the proximal epiphysis, the difference is quite small. We then used several different datasets to estimate the SVL and the TL of IVPP V 22770. The SVL estimates ranged from 313.23 to 512. 49 mm, with a TL estimate from 802.79 to 1254.87 mm (electronic supplementary material, table S9) based on a regression analysis from the combined data (Data S2) of Conrad *et al*. [5] and Schuett *et al*. [59].

Although the body form of Varanidae has been described as conservative [60], the extant species of *Varanus* are ecologically diverse (terrestrial, saxicolous, semi-aquatic and arboreal), and a study of *Varanus* showed that its species converged repeatedly on body plans and ecological niches [10].

Thompson & Withers [61] analysing the relative limb dimensions of 17 Australian *Varanus* suggested that they are morphologically diverse. They found a link between semi-aquatic habits and limb proportions, although the results were not conclusive [61]. Thompson *et al*. [62] later suggested a strong link between the body shape, as represented by morphometric characters such as body length and forelimb length, and the retreat preferences of *Varanus* spp. in Western Australia, and concluded that the morphometric disparity might be a combined effect of phylogeny, sex and ecology with body size also an important factor [62].

In *Archaeovaranus*, the forelimb length (FL; humerus + ulna) and hindlimb length (HL; femur + fibula) are similar (FL/HL proportion is 0.988), as are the humerus (H) and femur (F) (H/F proportion is 0.990). These proportions are not only outside the normal range of *Varanus* spp. (usually well below 1) but are also rare among limbed squamates generally [63], although these authors were unable to link these limb proportions to any particular lifestyle. The other Eocene stem-varanid *S. ensidens* resembles *Archaeovaranus* in being of medium-size [5], but has different proportions of the FL in relation to the HL (0.912) and of the H/F (0.853). This species was firstly interpreted as terrestrial based on its possession of a tail that is rounded rather than bilaterally compressed with tall neural spines, as might be expected in a swimmer [45]. By contrast, Rieppel & Grande [19] suggested the unfused astragalus and calcaneum in FMNH PR2378 could possibly indicate that *Saniwa* was semi-aquatic. These same authors also reported that body proportions placed *S. ensidens* FMNH PR 2378 between the arboreal *V. prasinus* and the

semi-aquatic *V. salvator*. However, although the data for *S. ensidens* remains inconclusive, the relatively longer forelimb in *Archaeovaranus* suggests the two species may have had different lifestyles.

(d) Bone histology of *Archaeovaranus lii* and the ontogenetic stage of the holotype

The timing of closure of the astragalocalcaneal suture in the ankle is variable among squamates, and an open suture may therefore be an age-dependent factor [64]. Our observation of the rib histology of the extant *V. salvator* shows an obvious decrease in growth rate near the periosteal surface (a broader layer of parallel-fibred bone indicated by the outer blueish region in the electronic supplementary material, figure S10B) in an individual with a clear astragalocalcaneal suture and indicates that the fusion between astragalus and calcaneum occurs late in *Varanus*, as Rieppel & Grande [19] argued.

The validity of growth marks in different bone elements of *Varanus* has been discussed by previous researchers [65]. The fibula usually retains more skeletal growth marks (SGMs) than the femur, tibia or phalanges in large individuals of *Varanus* [65], because the fibula bears less weight than other hindlimb bones and has less medullary resorption. We therefore chose the fibula in our study for age estimation, with the caveat that the fibula may appear to be older than other bone elements in a single skeleton [66].

Although a thin section of the right fibula (electronic supplementary material, figure S10A) indicated that its tissue had been partly modified by diagenesis, the principal bone tissue can still be recognized as parallel-fibred bone. The vascularization is very poor with no osteons present in the cortex, a condition similar to that in *Sphenodon punctatus* [67]. Most of the osteocyte lacunae are oval or nearly round with numerous canaliculi. Bone remodelling is very rare in the cortex, and no secondary osteons or endosteal bone were observed. Two types of SGMs, lines of arrested growth (LAGs) and annuli, were recognized and were used for the age estimation. The first SGM, which was defined as the 'neonatal line' by previous authors [65], is about 36 µm in diameter, and most of it has been resorbed by the medullary cavity. The second and third SGMs can be recognized as LAGs, because they are more birefringent than annuli under transmitted polarized light. The fourth to sixteenth SGMs are annuli with parallel-fibred tissue, and between these annuli are woven fibred primary periosteal tissue. A total of 16 SGMs are present in the cortex in IVPP V 22770, giving an age estimate of 16 years old for this individual. The spacing between the adjacent SGMs decreased dramatically after the fifth SGM, indicating that the growth rate dropped and reproductive maturity may have occurred at this age. The narrowing of intervals between the outer SGMs with no typical external fundamental system [68], indicates that this individual was still growing but at a very slow rate.

(e) The evolution of varanid cranial characters

The skull of extant species of *Varanus* is characterized by many distinctive features, including an elongated snout, posteriorly extended (retracted) external narial openings, median narial bar, cristae cranii that meet or nearly meet below the frontal, loss of a complete postorbital bar and development of an intramandibular joint. *Lanthanotus*, *Archaeovaranus* and *Saniwa* share the enlarged external narial openings and fused nasals, but differ from *Varanus* in having a complete postorbital bar and cristae cranii that do not meet in the midline (figure 3*a*). Thus, the midline contact of the cristae cranii to create a strong cylindrical frontal seems to coincide with the loss of the bony postorbital bar in the evolution of *Varanus* itself.

The South American teiid lizard *Salvator merrianae* is of similar size and lifestyle to *V. niloticus*, and the two species have a comparable bite force [69]. However, the skull of *Salvator* differs from that of *Varanus* in snout structure, and in having a complete postorbital bar and weakly developed cristae cranii on the frontal. Dutel *et al*. [69] found that the postorbital bar of *Salvator* experienced very high strain magnitudes during biting, especially in bites by the posterior teeth, and that removal of the bar significantly increased strain magnitudes in other parts of the skull. The postorbital bar is therefore important in maintaining skull integrity during biting in *Salvator*. Artificially modelling a postorbital bar on to *Varanus* decreased strain magnitudes across the skull to some degree, whereas removing the ventrally united cristae cranii (subolfactory processes) in the *Varanus* model significantly increased strain levels, particularly in the frontal. Extension and fusion of the cristae cranii in *Varanus* therefore strengthen the interorbital region of the skull, permitting loss of the postorbital bar without compromising skull rigidity [69]. The interorbital region experiences high levels of strain in *Varanus* during feeding movements like prey shaking and pull-back cutting that draws teeth through prey items [70]. A similar combination of cylindrical frontal and loss of the postorbital bar is seen in gekkotan lizards, where loss of the postorbital bar has been linked to increasing eye size and mesokinetic (frontoparietal) cranial kinesis [71]. The advantage to *Varanus* of losing the postorbital bar is less obvious as the eyes are not unusually large, and many varanids—especially the larger species—seem to have little or no kinesis [72]. However, loss of the bar may originally have been associated with mesokinesis, with subsequent loss or reduction of kinesis in some species, or it may have been secondary to strengthening the frontal, thereby helping to lighten the skull for fast inertial feeding, and create additional space for adductor muscles.

Saniwa and *Archaeovaranus* thus represent a stage of varanid evolution in which the long, fenestrated and flattened snout had already evolved, potentially increasing their ability to catch fast-moving prey [73], but without the strengthening of the frontal region and subsequent loss of the postorbital bar (figure 3*a*). In *Varanus*, the reduction of the tongue for a primarily sensory role, means that it can no longer be used for prey transport in the mouth and *Varanus* therefore uses inertial feeding [72]. However, the retention of palatal teeth in *Saniwa* and *Archaeovaranus* (lost in *Varanus*) is indicative of an interaction between the tongue and the palate in transferring prey towards the back of the mouth, suggesting the tongue of the extinct genera may have been fleshier, permitting lingual transport rather than inertial feeding. Unfortunately, very little information is available about the feeding behaviour of *Lanthanotus*, which also retains palatal teeth. The tongue is said to be divided into a thin, bifurcate anterior part [41] used, as in *Varanus*, for chemosensation, and a thicker posterior part. However, *Lanthanotus* has been observed to feed underwater, swallowing objects whole, but

not surfacing to use inertial feeding [74]. *Shinisaurus*, the extant sister taxon to *Lanthanotus* and *Varanus* [6], also has palatal (pterygoid) teeth and has been observed to use the tongue for intraoral transport, but not inertial feeding [75].

(f) The origin and palaeobiogeography of varanids

The divergence between lineages leading to *Varanus* and *Lanthanotus* has been dated to the mid-Cretaceous, around 80–100 Ma [10], and a recent estimate places the crown age of *Varanus* as early to middle Oligocene [10,76]. However, the earliest definitive *Varanus* remains are from the early Miocene [15,16] (figure 3*a*).

Several varaniform taxa (e.g. *Ovoo*, *Telmasaurus*, *Aiolosaurus*, *Saniwides and Proplatynota*) have been recorded from the Late Cretaceous deposits of the Gobi Desert [11–14], but their precise relationships to *Varanus* and *Lanthanotus* vary between published phylogenetic trees (e.g. [10,14,32,56]). In our analyses, all these taxa except *Cherminotus* were placed on the varanid stem. A second varaniform group has been described from the Palaeogene of Europe (Palaeovaranidae sensi [32,57]), but their proposed placement varies (sister to Lanthanotidae, [10]; or to Varanidae + Lanthanotidae, [32]), and our analyses did not recover it as a monophyletic group. The only Palaeogene taxon that had consistently been placed as a sister taxon to *Varanus* was *S. ensidens* from the Eocene of North America [18,19], although vertebrae referred to *Saniwa* or stem-*Varanus* have been reported from the earliest Eocene, or earlier middle Palaeocene to late Oligocene across North America, Europe, Africa and Asia [20,21,23,77–80].

Both molecular and morphological data support an Asian origin for Varanidae [5,8–10], although some researchers have presented molecular or palaeontological support for an African or Gondwanan origin [21,81]. A recent analysis [10] also placed the origin of varaniform lizards in East Asia with subsequent dispersal to Europe and North America, and the origin of *Varanus* was proposed to have followed a similar pattern. The discovery of *Ar. lii* from the early Eocene in central China suggests that the transition from Cretaceous varaniform lizards to *Varanus* could have occurred in East Asia before the origin and dispersal of *Varanus* to other regions took place. *Archaeovaranus* therefore fills a significant gap in the fossil record of varanids by clearly demonstrating the presence of a stem-varanid closely related to *Varanus* in the early Eocene of East Asia.

Data accessibility. The holotype specimen of *Archaeovaranus lii* IVPP V 22770 is deposited in the vertebrate collection of the Institute of Vertebrate Paleontology and Paleoanthropology, Chinese Academy of Sciences. The CT models and original data are available on the request of whoever is interested. The data matrix used for the phylogenetic analysis is included and uploaded as electronic supplementary material (data S1) [82].

Authors' contributions. All authors gave final approval for publication and agreed to be held accountable for the work performed therein.

Competing interests. We declare we have no competing interests.

Funding. This work was supported by the National Natural Science Foundation of China (grant nos 41688103, 42072031, 41702019), the Strategic Priority Research Program (B) of the Chinese Academy of Sciences (grant no. XDB 18000000), Youth Innovation Promotion Association (to D.L.P.), an Anne Sleep Award from the Linnaean Society of London in 2018 to allow D.L.P. to travel to London and Swiss National Science Foundation (grant no. 181041) to D.V.

Acknowledgements. The specimen was collected by Mr Wei Zhou, Mr Xun Jin and Mr Shijie Li, and prepared by Mr Shuhua Xie, Mr Long Xiang and Mrs Yanfang Guo to expose the bones, to detach the skull and the vertebrae from the block, and to prepare the fibula and ribs for histology. We are greatly indebted to these people. We are also grateful to Mr Wei Gao for photography, Mr Yemao Hou for scanning, and Ms Shukang Zhang for preparing the histological sections. We thank Dr Patrick Campbell for allowing one of us (D.L.P.) to check and measure specimens from the extant *Varanus* collection at the Natural History Museum, London, Dr Min Wang for discussion, Dr Jingsong Shi for extant *Varanus* and *Heloderma* disarticulated bones, and Dr Ryoko Matsumoto, Kanagawa Prefectural Museum of Natural History, for the CT scan of *Lanthanotus* donated to the Evans laboratory, UCL. We also thank the editor and reviewers for their helpful comments on early versions of the manuscript.

References

1. Auliya M, Koch A. 2020 Visual identification guide to the Monitor lizard species of the world (genus *Varanus*). *Bundesamt für Naturschutz*, BfN-Skripten 552.
2. Mertens R. 1942 Die Familie der Warane (Varanidae)–Teil 2, Der Schädel. *Abhandlungen der Senckenbergischen Naturforschenden Gesellschaft* **465**, 117–234.
3. Böhme W. 2003 Checklist of the living monitor lizards of the world (family Varanidae). *Zoologische Verhandelingen* **341**, 4–43.
4. Pianka ER, King D, King RA. 2004 *Varanoid lizards of the world*. Bloomington, IN: Indiana University Press.
5. Conrad JL, Balcarcel AM, Mehling CM. 2012 Earliest example of a giant monitor lizard (*Varanus*, Varanidae, Squamata). *PLoS ONE* **7**, e41767. (doi:10.1371/journal.pone.0041767)
6. Conrad JL. 2008 Phylogeny and systematics of Squamata (Reptilia) based on morphology. *Bull. Am. Mus. Natl Hist.* **310**, 1–182. (doi:10.1206/310.1)
7. Gauthier JA, Kearney M, Maisano JA, Rieppel O, Behlke ADB. 2012 Assembling the squamate tree of life: perspectives from the phenotype and the fossil record. *Bull. Peabody Mus. Natl Hist.* **53**, 3–308. (doi:10.3374/014.053.0101)
8. Estes R. 1983 *Sauria Terrestria, Amphisbaenia. Encyclopedia of paleoherpetology, part 10A*. Stuttgart, Germany: Gustav Fischer Verlag.
9. Vidal N *et al.* 2012 Molecular evidence for an Asian origin of monitor lizards followed by Tertiary dispersals to Africa and Australasia. *Biol. Lett.* **8**, 853–855. (doi:10.1098/rsbl.2012.0460)
10. Brennan IG, Lemmon AR, Lemmon EM, Portik DM, Weijola V, Welton L, Donnellan SC, Keogh JS. 2021 Phylogenomics of monitor lizards and the role of competition in dictating body size disparity. *Syst. Biol.* **70**, 120–132. (doi:10.1093/sysbio/syaa046)
11. Gilmore CW. 1943 Fossil lizards of Mongolia. *Bull. Am. Mus. Natl Hist.* **81**, 361–384.
12. Borsuk-Białynicka M. 1984 Anguimorphans and related lizards from the Late Cretaceous of the Gobi Desert, Mongolia. *Palaeontol. Polonica* **46**, 5–105.
13. Gao K, Norell MA. 2000 Taxonomic composition and systematics of Late Cretaceous lizard assemblages from Ukhaa Tolgod and adjacent localities, Mongolian Gobi Desert. *Bull. Am. Mus. Natl Hist.* **249**, 1–118. (doi:10.1206/0003-0090(2000)249<0001:TCASOL>2.0.CO;2)
14. Norell MA, Gao KQ, Conrad J. 2007 A new platynotan lizard (Diapsida: Squamata) from the Late Cretaceous Gobi Desert (Ömnögov), Mongolia. *Am. Mus. Novitates* **3605**, 1–22. (doi:10.1206/0003-0082(2008)3605[1:ANPLDS]2.0.CO;2)

15. Clos LM. 1995 A new species of *Varanus* (Reptilia: Sauria) from the Miocene of Kenya. *J. Vertebr. Paleontol.* **15**, 254–267. (doi:10.1080/02724634.1995.10011228)
16. Ivanov M, Ruta M, Klembara J, Böhme M. 2017 A new species of *Varanus* (Anguimorpha: Varanidae) from the early Miocene of the Czech Republic, and its relationships and palaeoecology. *J. Syst. Paleontol.* **16**, 767–797. (doi:10.1080/14772019.2017.1355338)
17. Villa A *et al.* 2018 Revision of *Varanus marathonensis* (Squamata, Varanidae) based on historical and new material: morphology, systematics, and paleobiogeography of the European monitor lizards. *PLoS ONE* **13**, e0207719. (doi:10.1371/journal.pone.0207719)
18. Gilmore CW. 1928 Fossil lizards of North America. *Mem. Natl Acad. Sci.* **22**, 1–201.
19. Rieppel O, Grande L. 2007 The anatomy of the fossil varanid lizard *Saniwa ensidens* Leidy, 1870, based on a newly discovered complete skeleton. *J. Paleontol.* **81**, 643–665. (doi:10.1666/pleo0022-3360(2007)081[0643:TAOTFV]2.0.CO;2)
20. Smith KT, Bhullar B-AS, Holroyd PA. 2008 Earliest African record of the *Varanus* stem-clade (Squamata: Varanidae) from the early Oligocene of Egypt. *J. Vertebr. Paleontol.* **28**, 909–913. (doi:10.1671/0272-4634(2008)28[909:EAROTV]2.0.CO;2)
21. Holmes RB, Murray AM, Attia YS, Simons EL, Chatrath P. 2010 Oldest known *Varanus* (Squamata: Varanidae) from the Upper Eocene and Lower Oligocene of Egypt: support for an African origin of the genus. *Palaeontology* **53**, 1099–1110. (doi:10.1111/j.1475-4983.2010.00994.x)
22. Alifanov V. 1993 Some peculiarities of the Cretaceous and Palaeogene lizard faunas of the Mongolian People's Republic. *Kaupia – Darmstädter Beiträge zur Naturgeschichte* **3**, 9–13.
23. Dong L, Evans SE, Wang Y. 2016 Taxonomic revision of lizards from the Paleocene deposits of the Qianshan Basin, Anhui, China. *Vertebrata PalAsiatica* **54**, 243–268.
24. Ma A, Cheng J. 1991 On biostratigraphical subdivision of Yuhuangding Formation in Liguanqian Basin of Eastern Qinling Region. *Sci. Geol. Sin.* **1991**, 21–29. (in Chinese).
25. Wang Y, Li Q, Bai B, Jin X, Mao F, Meng J. 2019 Paleogene integrative stratigraphy and timescale of China. *Sci. China Earth Sci.* **62**, 287–309.
26. Wang Y. 1995 A new primitive chalicothere (Perissodactyla, Mammalia) from the early Eocene of Hubei. China. *Vertebrata PalAsiatica* **33**, 138–159. (in Chinese). (doi:10.1007/s11430-018-9305-y)
27. Zhu M, Ding Z, Wang X, Chen Z, Jiang H, Dong X, Ji J, Tang Z, Luo P. 2010 High-resolution carbon isotope record for the Paleocene-Eocene Thermal Maximum from the Nanyang Basin, Central China. *Chin. Sci. Bull.* **55**, 3606–3611. (doi:10.1007/s11434-010-4092-5)
28. Chen Z, Wang X, Hu J, Yang S, Zhu M, Dong X, Tang Z, Ding Z. 2014 Structure of the carbon isotope excursion in a high-resolution lacustrine Paleocene–Eocene Thermal Maximum record from central China. *Earth Planet. Sci. Lett.* **408**, 331–340. (doi:10.1016/j.epsl.2014.10.027)
29. Chen Z, Ding Z, Yang S, Zhang C, Wang X. 2016 Increased precipitation and weathering across the Paleocene-Eocene Thermal Maximum in central China. *Geochem. Geophys. Geosyst.* **17**, 2286–2297. (doi:10.1002/2016GC006333)
30. Sun X, Wang P. 2005 How old is the Asian monsoon system?—Palaeobotanical records from China. *Palaeogeogr. Palaeoclimatol. Palaeoecol.* **222**, 181–222. (doi:10.1016/j.palaeo.2005.03.005)
31. Conrad JL, Ast JC, Montanari S, Norell MA. 2011 A combined evidence phylogenetic analysis of Anguimorpha (Reptilia: Squamata). *Cladistics* **27**, 230–277. (doi:10.1111/j.1096-0031.2010.00330.x)
32. Smith KT, Habersetzer J. 2021 The anatomy, phylogenetic relationships, and autecology of the carnivorous lizard '*Saniwa*' *feisti* Stritzke, 1983 from the Eocene of Messel, Germany. *Comptes Rendus Palevol*. **20**, 441–506. (dol:10.5852/cr-palevol2021v20a23)
33. Pyron RA, Burbrink FT, Wiens JJ. 2013 A phylogeny and revised classification of Squamata, including 4161 species of lizards and snakes. *BMC Evol. Biol.* **13**, Art.93. (doi:10.1186/1471-2148-13-93)
34. Goloboff PA, Catalano SA. 2016 TNT version 1.5, including a full implementation of phylogenetic morphometrics. *Cladistics* **32**, 221–238. (doi:10.1111/cla.12160)
35. Jiang H, Zhong N, Li Y, Xu H, Ma X, Meng Y, Mao X. 2014 Magnetostratigraphy and grain size record of the Xijiadian fluviolacustrine sediments in East China and its implied stepwise enhancement of the westerly circulation during the Eocene period. *J. Geophys. Res.* **119**, 7442–7457. (doi:10.1002/2014JB011225)
36. de Buffrénil V, Ineich I, Böhme W. 2004 Comparative data on epiphyseal development in the family Varanidae. *J. Herpetol.* **37**, 328–335. (doi:10.1670/0022-1511(2005)039[0328:CDOEDI]2.0.CO;2)
37. Estes R, Queiroz KD, Gauthier J. 1988 Phylogenetic relationships within Squamata. In *Phylogenetic relationships of the lizard families—essays commemorating Charles L. Camp* (eds R Estes, G Pregill), pp. 119–281. Stanford, CA: Stanford University Press.
38. Evans SE. 2008 The skull of lizards and Tuatara. In *The skull of lepidosauria, vol. 20, morphology H* (eds G Gans, AS Gaunt, K Adler), pp. 1–344. New York, NY: Ithaca.
39. Bellairs A. 1949 Observations on the snout of *Varanus*, and a comparison with that of other lizards and snakes. *J. Anat.* **83**, 116–146.
40. Oelrich TM. 1956 The anatomy of the head of *Ctenosaura pectinata* (Iguanidae). *Miscellaneous publications, Museum of Zoology, University of Michigan*, No. 94, 122.
41. McDowell JSB, Bogert CM. 1954 The systematic position of *Lanthanotus* and the affinities of the anguimorphan lizards. *Bull. Am. Mus. Natl Hist.* **105**, 1–142.
42. The Deep Scaly Project. 2011 '*Lanthanotus borneensis*' (On-line), Digital Morphology. Accessed 7 August 2021 at http://digimorph.org/specimens/Lanthanotus_borneensis/ATOL/.
43. Werneburg I, Polachowski KM, Hutchinson MN. 2015 Bony skull development in the Argus monitor (Squamata, Varanidae, *Varanus panoptes*) with comments on developmental timing and adult anatomy. *Zoology (Jena)* **118**, 255–280. (doi:10.1016/j.zool.2015.02.004)
44. Rieppel O, Gauthier J, Maisano J. 2008 Comparative morphology of the dermal palate in squamate reptiles, with comments on phylogenetic implications. *Zool. J. Linn. Soc.* **152**, 131–152. (doi:10.1111/j.1096-3642.2007.00337.x)
45. Gilmore CW. 1922 A new description of *Saniwa ensidens* Leidy, an extinct varanid lizard from Wyoming. *Proc. US Natl Mus.* **60**, 1–31. (doi:10.5479/si.00963801.60-2418.1)
46. Norell M, Gao K. 1997 Braincase and phylogenetic relationships of *Estesia mongoliensis* from the Late Cretaceous of the Gobi Desert and the recognition of a new clade of lizards. *Am. Mus. Novitates* **1132**, 1–25.
47. Head JJ, Barrett PM, Rayfield EJ. 2009 Neurocranial osteology and systematic relationships of *Varanus* (*Megalania*) *prisca* Owen, 1859 (Squamata: Varanidae). *Zool. J. Linn. Soc.* **155**, 445–457. (doi:10.1111/j.1096-3642.2008.00448.x)
48. Rieppel O. 1983 A comparison of the skull of *Lanthanotus borneensis* (Reptilia: Varanoidea) with the skull of primitive snakes. *Zeitschrift für Zoologische Systematik und Evolutionsforschung* **21**, 142–153. (doi:10.1111/j.1439-0469.1983.tb00282.x)
49. Cieri RL. 2018 The axial anatomy of monitor lizards (Varanidae). *J. Anat.* **233**, 636–643. (doi:10.1111/joa.12872)
50. Rieppel O. 1980 The postcranial skeleton of *Lanthanotus borneensis* (Reptilia, Lacertilia). *Amphibia-Reptilia* **1**, 95–112. (doi:10.1163/156853880X00105)
51. Georgalis GL, Abdel Gawad MK, Hassan SM, El-Barkooky AN, Hamdan MA. 2020 Oldest co-occurrence of *Varanus* and *Python* from Africa—first record of squamates from the early Miocene of Moghra Formation, Western Desert, Egypt. *PeerJ* **8**, e9092. (doi:10.7717/peerj.9092)
52. Hoffstetter R. 1969 Presence de Varanidae (Reptilia, Sauria) dans le Miocene de Catalogne. Considerations sur l'histoire de la famille. *Bull. du Muséum national d'Histoire naturelle* **40**, 1051–1064.
53. Reeder TW, Townsend TM, Mulcahy DG, Noonan BP, Wood PL, Sites JW, Wiens JJ. 2015 Integrated analyses resolve conflicts over squamate reptile phylogeny and reveal unexpected placements for fossil taxa. *PLoS ONE* **10**, e0118199. (doi:10.1371/journal.pone.0118199)
54. Simões TR, Vernygora O, Paparella I, Jimenez-Huidobro P, Caldwell MW. 2017 Mosasauroid phylogeny under multiple phylogenetic methods provides new insights on the

evolution of aquatic adaptations in the group. *PLoS ONE* **12**, e0176773. (doi:10.1371/journal.pone.0176773)

55. Lee MSY. 1997 The phylogeny of varanoid lizards and the affinities of snakes. *Phil. Trans. R. Soc. Lond. B* **352**, 53–91. (doi:10.1098/rstb.1997.0005)
56. Conrad JL, Grande L, Rieppel O. 2008 Re-assessment of varanid evolution based on new data from *Saniwa ensidens* Leidy, 1870 (Squamata, Reptilia). *Am. Mus. Novitates* **3630**, 1–16. (doi:10.1206/596.1)
57. Georgalis GL. 2017 *Necrosaurus* or *Palaeovaranus?* Appropriate nomenclature and taxonomic content of an enigmatic fossil lizard clade (Squamata). *Ann. de Paléontologie* **103**, 293–303. (doi:10.1016/j.annpal.2017.10.001)
58. Burbrink FT *et al.* 2020 Interrogating genomic-scale data for Squamata (lizards, snakes, and amphisbaenians) shows no support for key traditional morphological relationships. *Syst. Biol.* **69**, 502–520. (doi:10.1093/sysbio/syz062)
59. Schuett GW, Reiserer RS, Earley RL. 2009 The evolution of bipedal postures in varanoid lizards. *Biol. J. Linn. Soc.* **97**, 652–663. (doi:10.1111/j.1095-8312.2009.01227.x)
60. Pianka ER. 1995 Evolution of body size: varanid lizards as a model system. *Am. Nat.* **146**, 398–414. (doi:10.1086/285806)
61. Thompson GG, Withers PC. 1997 Comparative morphology of western Australian varanid lizards (Squamata: Varanidae). *J. Morphol.* **233**, 127–152. (doi:10.1002/(SICI)1097-4687(199708)233:2<127::AID-JMOR4>3.0.CO;2-3)
62. Thompson GG, Clemente CJ, Withers PC, Fry BG, Norman JA. 2008 Is body shape of varanid lizards linked with retreat choice. *Aust. J. Zool.* **56**, 351. (doi:10.1071/ZO08030)
63. Villaseñor-Amador D, Suárez NX, Alberto Cruz J. 2021 Bipedalism in Mexican Albian lizard (Squamata) and the locomotion type in other Cretaceous lizards. *J. South Am. Earth Sci.* **109**. 103299. (doi:10.1016/j.jsames.2021.103299)
64. Russell AP, Bauer AM. 2008 The appendicular locomotor apparatus of *Sphenodon* and normal-limbed squamates. In *The skull and appendicular locomotor apparatus of lepidosauria,* vol. 21, *morphology I* (eds C Gans, AS Gaunt, A Kraig), pp. 1–466. New York, NY: Ithaca.
65. de Buffrénil V, Castanet J. 2000 Age estimation by skeletochronology in the Nile monitor (*Varanus niloticus*), a highly exploited species. *J. Herpetol.* **34**, 414–424. (doi:10.2307/1565365)
66. Zhao Q, Benton M, Hayashi S, Xu X. 2019 Long bone histology and growth patterns of *Psittacosaurus lujiatunensis* (Dinosauria: Ceratopsia). *Acta Palaeontol. Polonica* **64**, 323–334. (doi:10.4202/app.00559.2018)
67. Scheyer TM, Klein N, Sander PM. 2010 Developmental palaeontology of Reptilia as revealed by histological studies. *Seminars Cell Dev. Biol.* **21**, 462–470. (doi:10.1016/j.semcdb.2009.11.005)
68. Cormack D. 1987 *Ham's histology*, 732 p. New York, NY: Lippincott.
69. Dutel H, Gröning F, Sharp AC, Watson PJ, Herrel A, Ross CF, Jones ME, Evans SE, Fagan MJ. 2021 Comparative cranial biomechanics in two lizard species: impact of variation in cranial design. *J. Exp. Biol.* **224**, jeb234831. (doi:10.1242/jeb.234831)
70. McCurry MR, Mahony M, Clausen PD, Quayle MR, Walmsley CW, Jessop TS, Wroe S, Richards H, McHenry CR. 2015 The relationship between cranial structure, biomechanical performance and ecological diversity in varanoid lizards. *PLoS ONE* **10**, e0130625. (doi:10.1371/journal.pone.0130625)
71. Herrel A, Aerts P, De Vree F. 2000 Cranial kinesis in geckoes: functional implications. *J. Exp. Biol.* **203**, 1415–1423. (doi:10.1242/jeb.203.9.1415)
72. Herrel A, Schaerlaeken V, Meyers JJ, Metzger KA, Ross CF. 2007 The evolution of cranial design and performance in squamates: consequences of skull-bone reduction on feeding behavior. *Integr. Comp. Biol.* **47**, 107–117. (doi:10.1093/icb/icm014)
73. Metzger KA, Herrel A. 2005 Correlations between lizard cranial shape and diet: a quantitative, phylogenetically informed analysis. *Biol. J. Linn. Soc.* **86**, 433–466. (doi:10.1111/j.1095-8312.2005.00546.x)
74. Mendyk RW, Shuter A, Kalkriner A. 2015 Historical notes on a living specimen of *Lanthanotus borneensis* (Squamata: Sauria: Lanthanotidae) maintained at the Bronx Zoo from 1968 to 1976. *Biawak* **9**, 44–49.
75. Tchobanov R. 2015 Nahrungsaufnahme bei *Shinisaurus crocodilurus* (Ahl, 1930). Masters thesis, University of Vienna, Vienna, Austria. See http://othes.univie.ac.at/37959/1/2015-06-22_0706601.pdf.
76. Lin L, Wiens JJ. 2017 Comparing macroecological patterns across continents: evolution of climatic niche breadth in varanid lizards. *Ecography* **40**, 960–970. (doi:10.1111/ecog.02343)
77. Augé M. 1990 *La faune de lezards et d'amphisbaenes (Reptilia, Squamata) du gisement de Dormaal (Belgique, Eocene inferieur) (60)*. Bruxelles, Belgique: Institut Royal des Sciences naturelles de Belgique.
78. Smith KT. 2009 A new lizard assemblage from the earliest Eocene (Zone Wa0) of the Bighorn Basin, Wyoming, USA: biogeography during the warmest interval of the Cenozoic. *J. Syst. Paleontol.* **7**, 299–358. (doi:10.1017/S1477201909002752)
79. Zerova GA, Chkhikvadze VM. 1986 Neogene varanids of the USSR. Studies in Herpetology. In *Proc. of the European Herpetological Meeting* (ed. Z Rocek), *Prague*, *1985*, pp. 689–694. Prague, Czech Republic: Charles University.
80. Averianov AO, Danilov IG. 1997 A varanid lizard (Squamata: Varanidae) from the Early Eocene of Kirghizia. *Russian J. Herpetol.* **4**, 143–147. (doi:10.30906/1026-2296-1997-4-2-143-147)
81. Schulte JA, Melville J, Larson A. 2003 Molecular phylogenetic evidence for ancient divergence of lizard taxa on either side of Wallace's Line. *Proc. R. Soc. Lond. B* **270**, 597–603. (doi:10.1098/rspb.2002.2272)
82. Dong L, Wang Y-Q, Zhao Q, Vasilyan D, Wang Y, Evans SE. 2022 A new stem-varanid lizard (Reptilia, Squamata) from the early Eocene of China. Figshare.